Electronic Supplementary Information

The Contradictory Effect of the Methoxy-Substituent in Palladium-Catalyzed Ethylene/Methyl acrylate Copolymerization

V. Rosar,[a,b,c] A. Meduri,[a,d,*] T. Montini,[a,e] P. Fornasiero,[a,e] E. Zangrando,[a,*] and B. Milani[a,*]

Contents:

[a.] *Department of Chemical and Pharmaceutical Sciences, University of Trieste, Via Licio Giorgieri, 1, 34127 Trieste, Italy. Email: milaniba@units.it; Fax: +39 040 5583903; Tel.: +39 040 5583956.*
[b.] *Dr. V. Rosar, Consorzio Interuniversitario per la Reattività Chimica e la Catalisi CIRCC, Via Celso Ulpiani 27, 70126 Bari, Italy.*
[c.] *Current address: Department of Chemistry and Biochemistry, University of Bern, Freiestrasse 3, 3012 Bern, Switzerland.*
[d.] *Current address: RINA Consulting - Centro Sviluppo Materiali S.p.A., Materials, Technology & Innovation, Zona Ind. S. Pietro Lametino, 88046 Lamezia Terme (CZ) Italy.*
[e.] *National Interuniversity Consortium of Materials Science and Technology (INSTM) Trieste Research Unit and ICCOM-CNR Trieste Research Unit.*

X-Ray crystallography. Data collection of **1a** was performed at the X-ray diffraction beamline (XRD1) of the Elettra Synchrotron (Trieste, Italy), with a Pilatus 2M image plate detector. Complete dataset was collected at 100 K with a monochromatic wavelength of 0.700 Å, through the rotating crystal method. The diffraction data were indexed, integrated and scaled using XDS [1]. The structure was solved by direct methods using SIR2014 [2] and subsequent Fourier analysis and refinement with the full-matrix least-squares method based on F^2 were performed with SHELXL [3]. The asymmetric unit contains a CH_2Cl_2 solvent molecule. One CF_3 group was found disordered over two positions (occupancy of 0.59(1)/0.41(1)) and was refined with geometrical restraints. Hydrogen atoms were included at calculated positions. All the calculations were performed using the WinGX System, Ver 2013.3 [4]. Crystal data and details of refinements are given in Table S1.

[1] W. Kabsch, Acta Cryst. D 66 (2010) 125-132.
[2] M.C. Burla, R. Caliandro, B. Carrozzini, G.L. Cascarano, C. Cuocci, C. Giacovazzo, M. Mallamo, A. Mazzone, G.J. Polidori, Appl. Cryst. 48 (2015) 306-309.
[3] G.M. Sheldrick, Acta Cryst. A64 (2008) 112-122.
[4] Farrugia, L. J. (2012). J. Appl. Cryst. 45, 849-854

Table S1. Crystallographic data and details of the refinement for compound **1a.**

Empirical formula	$C_{30}H_{23}Cl_3F_6N_2OPd$
Formula weight	754.25
Temperature	100(2) K
Wavelength	0.7000 Å
Crystal system	Orthorhombic
Space group	*P* bca
Unit cell dimensions	*a*=15.550(2) *b*=19.500(2) *c*=20.140(1) Å
Volume	6107.0(11) $Å^3$
Z, Calculated density	8, 1.641 Mg/m^3
Absorption coefficient	0.811 mm^{-1}
F(000)	3008
Crystal size	0.34 x 0.34 x 0.30
Theta range for data collection	1.93 - 29.31°
Limiting indices	0<=h<=21, 0<=k<=27, 0<=l<=28
Reflections collected/ unique	68905/ 8735 [*R*(int) = 0.0508]
Completeness to theta 24.83°	99.9%
Refinement method	Full-matrix least-squares on F^2
Data/ restraints/ parameters	8735/ 39/ 402
Goodness-of-fit on F^2	1.069
Final R indices[I>2sigma(I)]	*R*1=0.0741, *wR*2=0.2010
R indices (all data)	*R*1=0.0791, *wR*2=0.2049
Extinction coefficient	0.0083(5)
Largest diff. peak and hole	2.277, -1.498 e.$Å^{-3}$

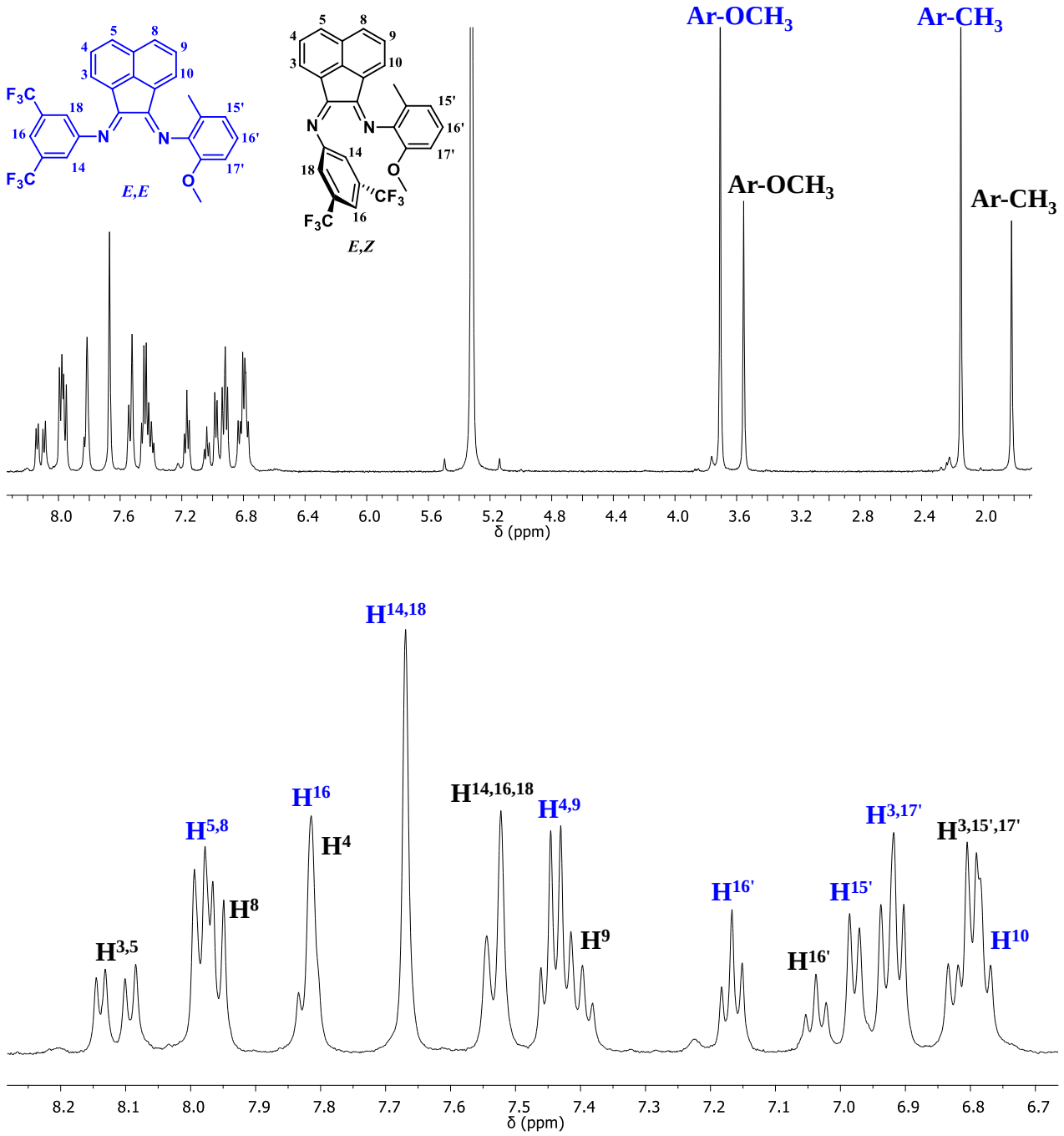

Figure S1. ^{1}H NMR spectrum of ligand **1** in CD_2Cl_2 at 298 K (top), enlargement of the aromatic region (below). *E*,*E* (blue) and *E*,*Z* (black) isomers.

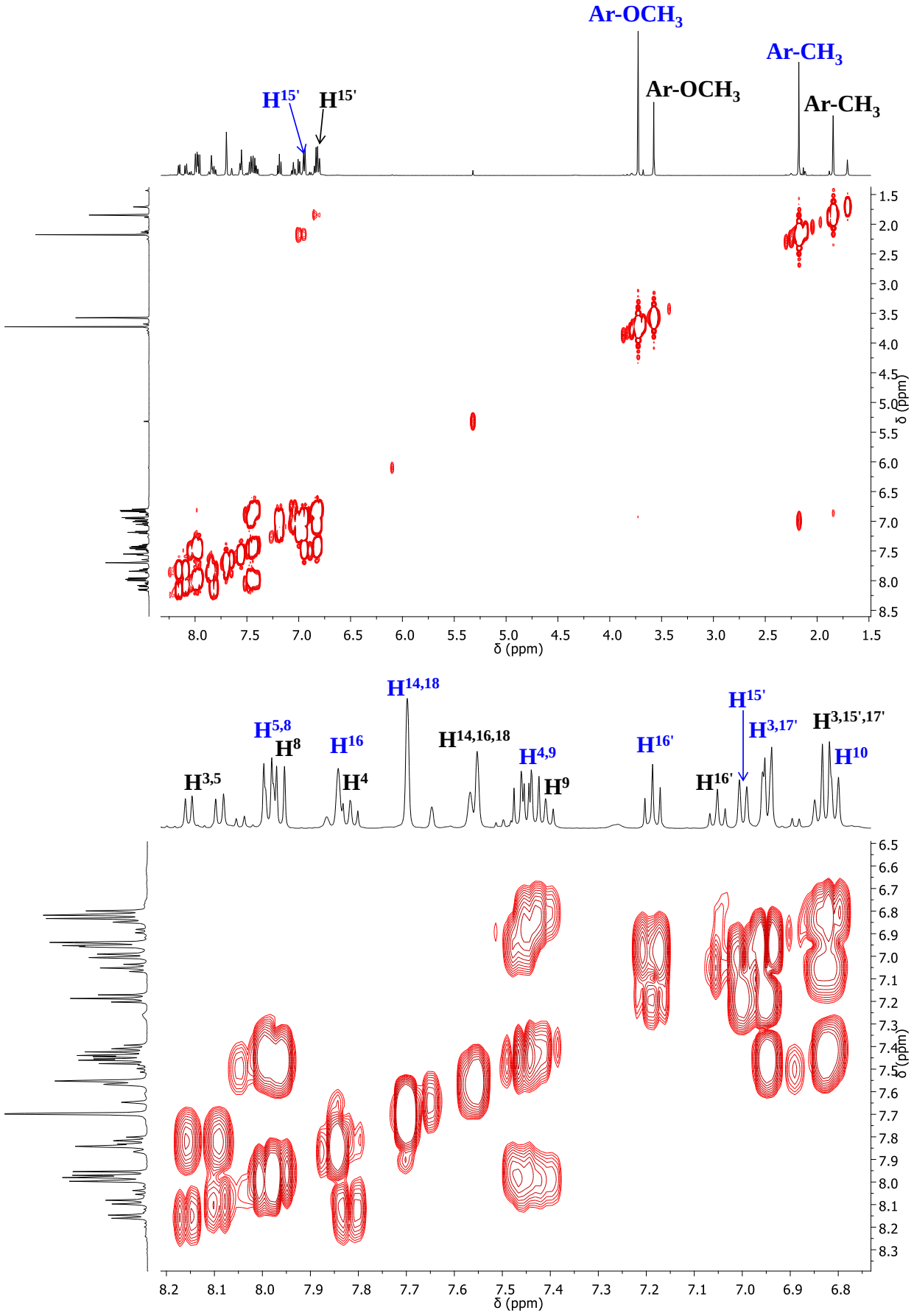

Figure S2. {^{1}H,^{1}H}-COSY spectrum of ligand **1** in CD_2Cl_2 at 298 K (top); region of aromatic protons (below).

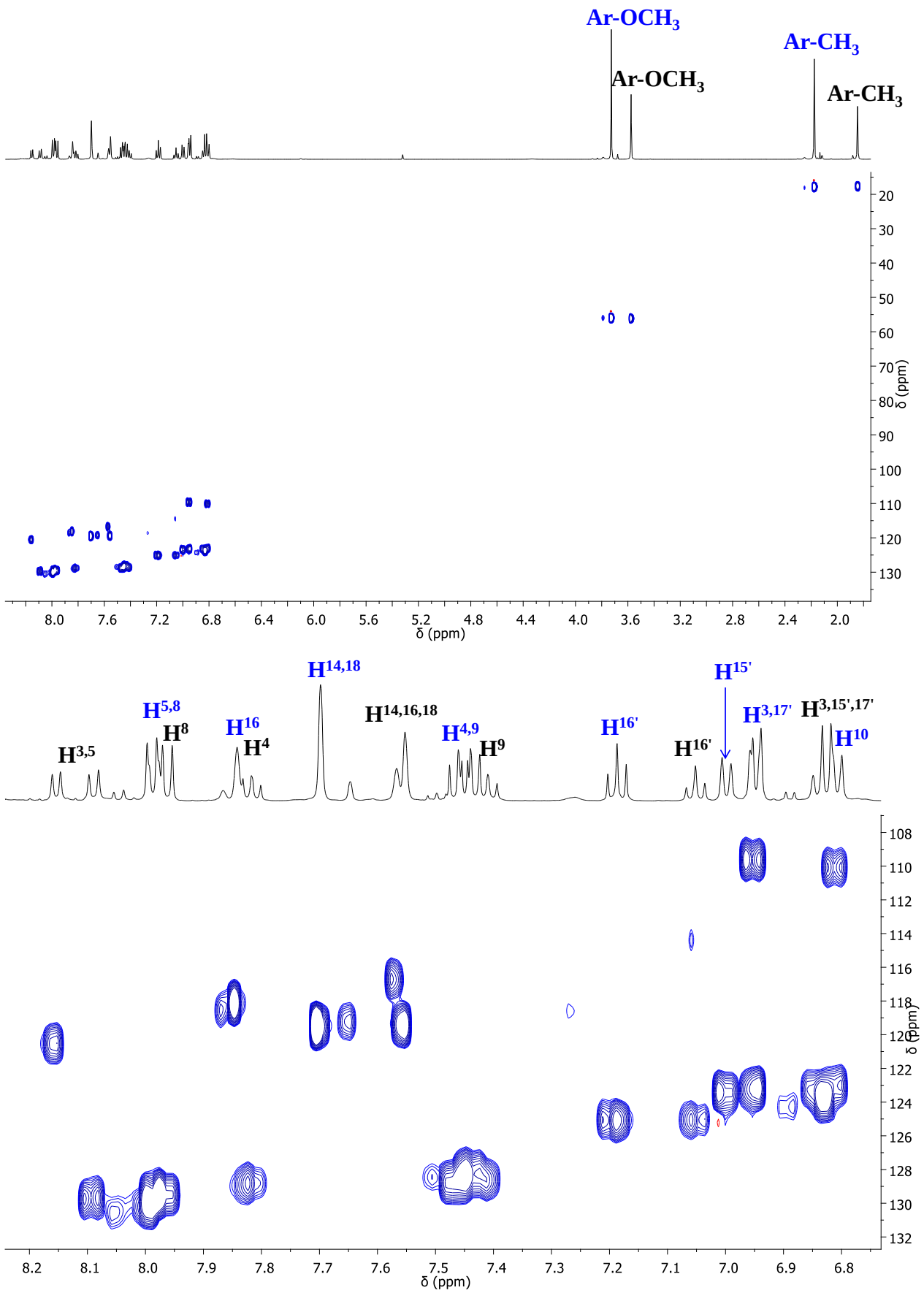

Figure S3. {^{1}H,^{13}C}-HSQC spectrum of ligand **1** in CD_2Cl_2 at 298 K (top); region of aromatic carbons (below).

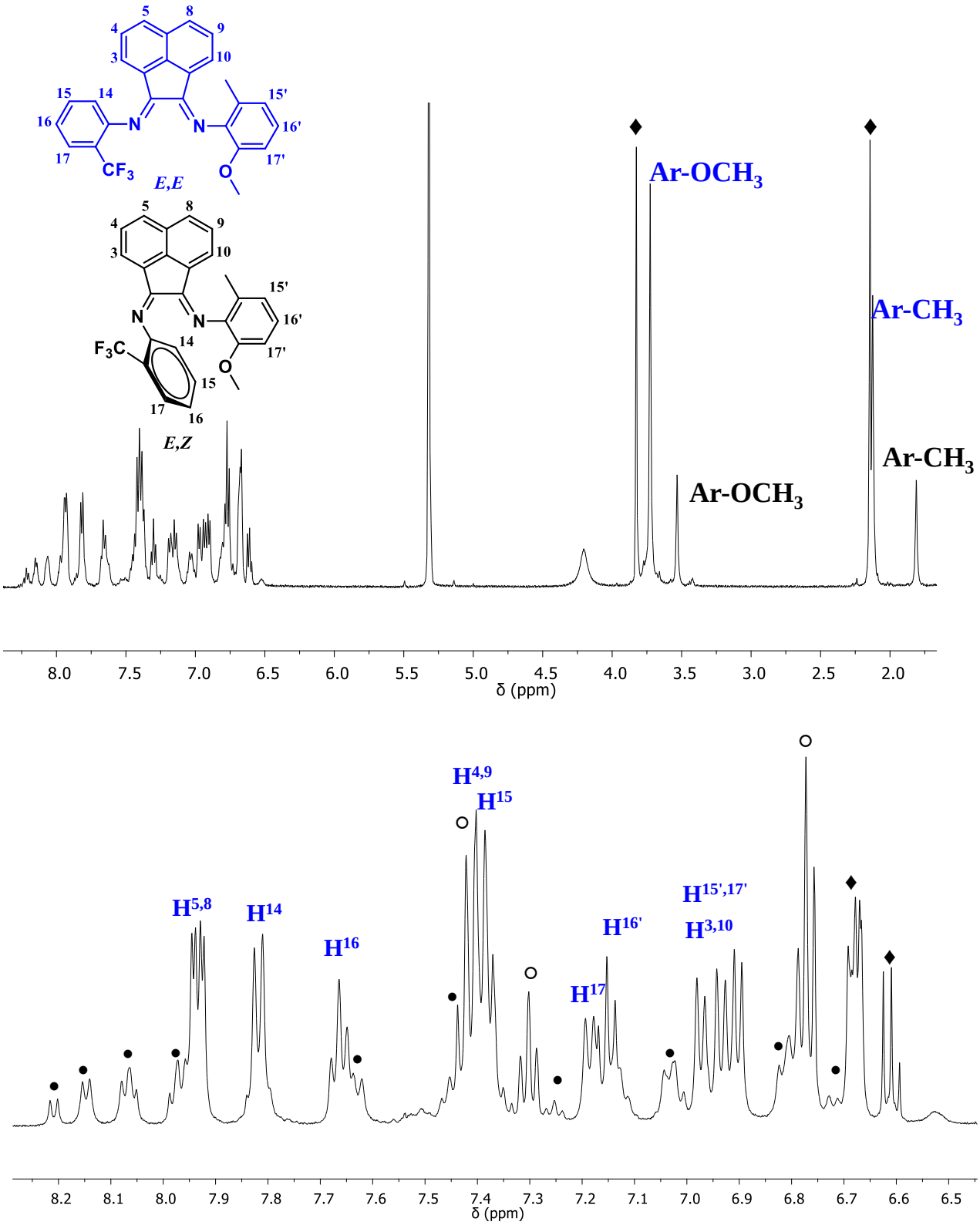

Figure S4. ^{1}H NMR spectrum of ligand **2** in CD_2Cl_2 at 298 K (top), enlargement of the aromatic region (bottom). *E,E* (blue) and *E,Z* (black) isomers. ♦ 2-methoxy-6-methylaniline; ○ 2-trifluoromethylaniline.

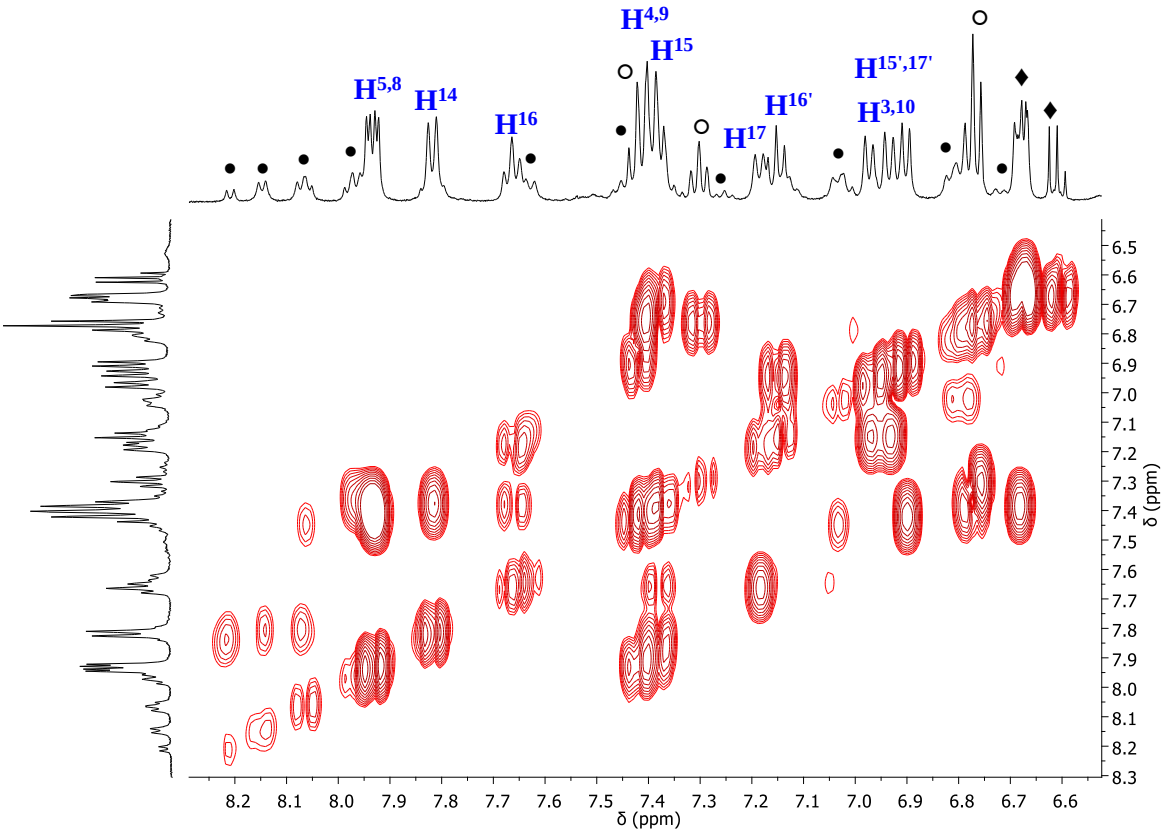

Figure S5. {^{1}H,^{1}H}-COSY spectrum of ligand **2** in CD_2Cl_2 at 298 K; region of aromatic protons. *E*,*E* (blue) and *E*,*Z* (black) isomers. ♦ 2-methoxy-6-methylaniline; ○ 2-trifluoromethylaniline.

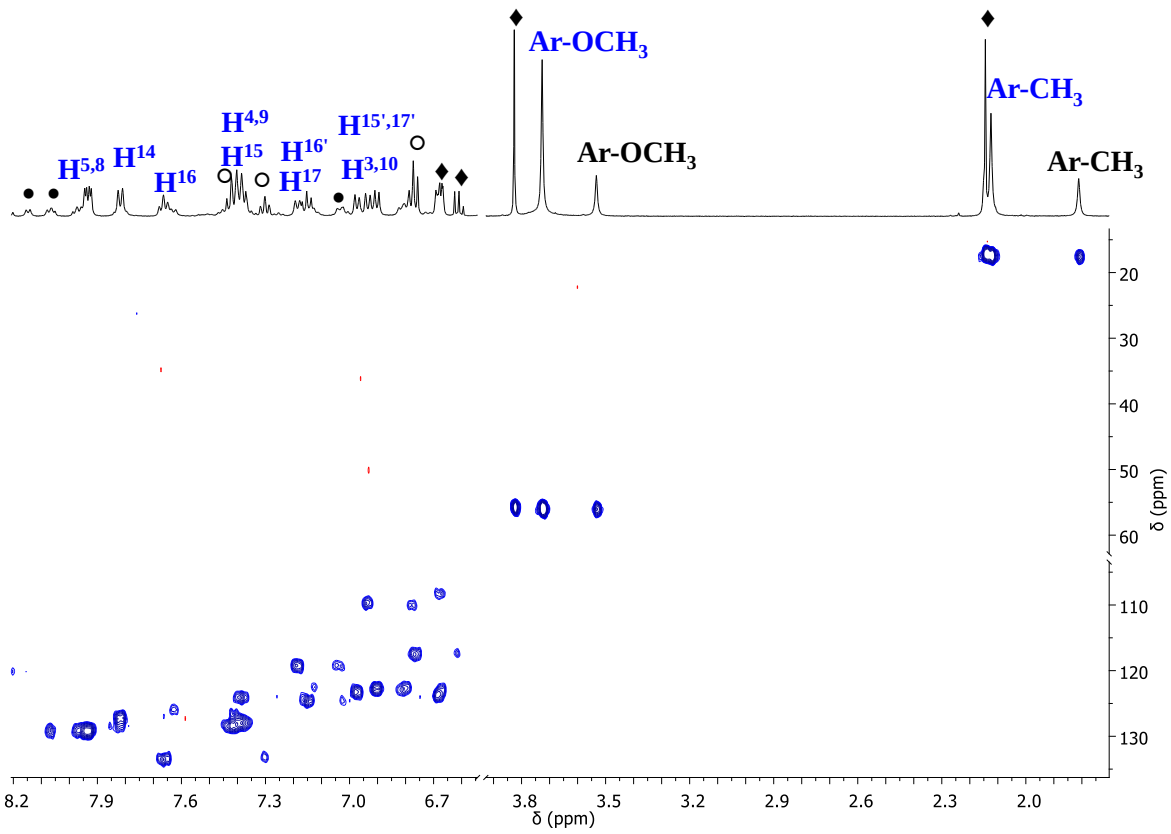

Figure S6. {^{1}H,^{13}C}-HSQC spectrum of ligand **2** in CD_2Cl_2 at 298 K. *E*,*E* (blue) and *E*,*Z* (black) isomers. ♦ 2-methoxy-6-methylaniline; ○ 2-trifluoromethylaniline.

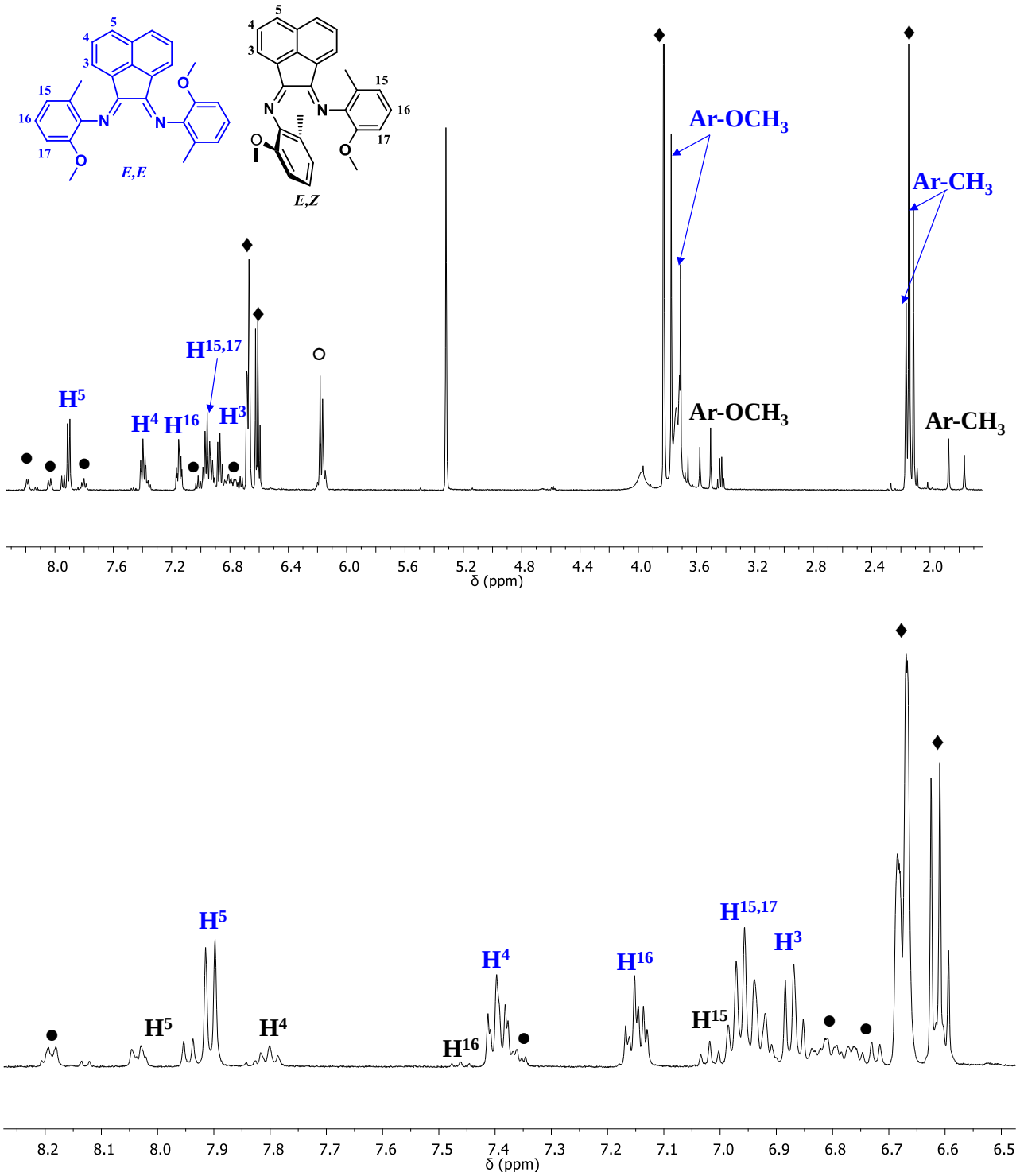

Figure S7. ^{1}H NMR spectrum of ligand **3** in CD_2Cl_2 at 298 K (top), enlargement of the aromatic region (bottom). *E,E* (blue) and *E,Z* (black) isomers. ♦ 2-methoxy-6-methylaniline; ○ 3,5-fluoroaniline.

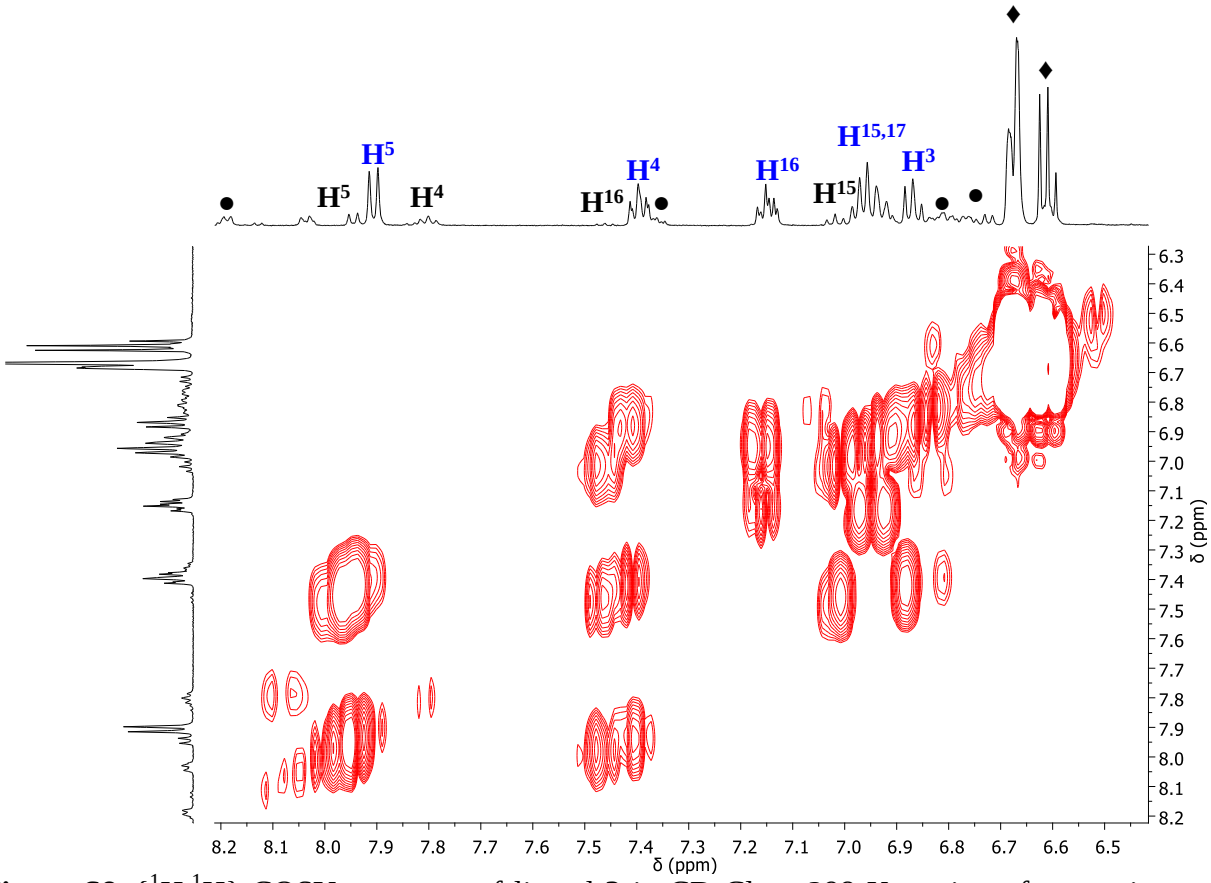

Figure S8. {^{1}H,^{1}H}-COSY spectrum of ligand **3** in CD_2Cl_2 at 298 K; region of aromatic protons. *E*,*E* (blue) and *E*,*Z* (black) isomers. ♦ 2-methoxy-6-methylaniline.

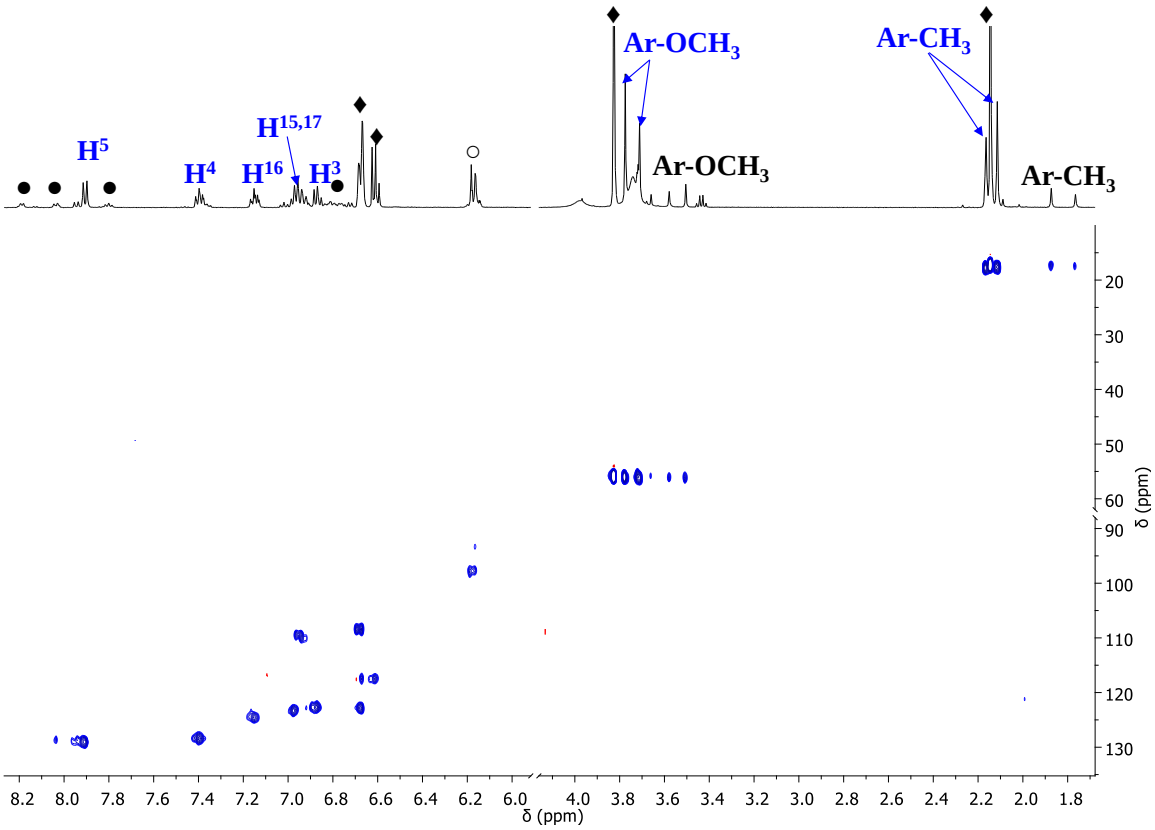

Figure S9. {^{1}H,^{13}C}-HSQC spectrum of ligand **3** in CD_2Cl_2 at 298 K. *E*,*E* (blue) and *E*,*Z* (black) isomers. ♦ 2-methoxy-6-methylaniline; ○ 3,5-fluoroaniline.

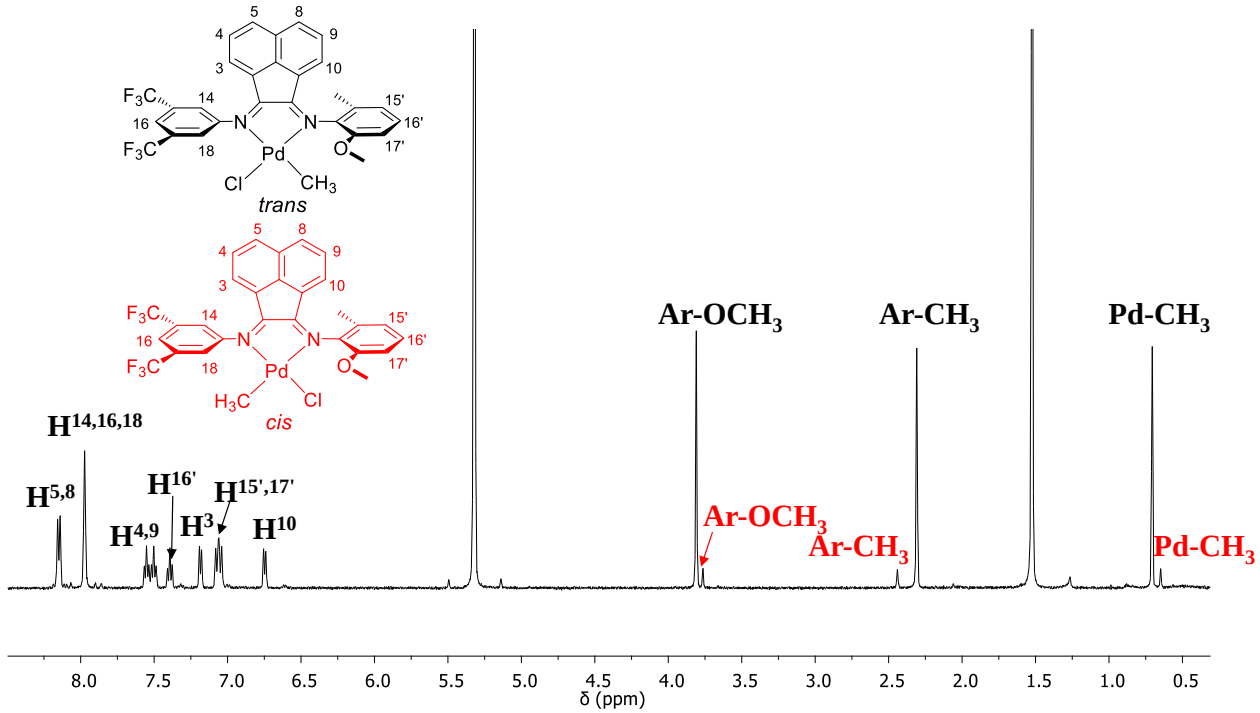

Figure S10. ^{1}H NMR spectrum of complex **1a** in CD_2Cl_2 at 298 K. *trans* (black) and *cis* (red) isomers.

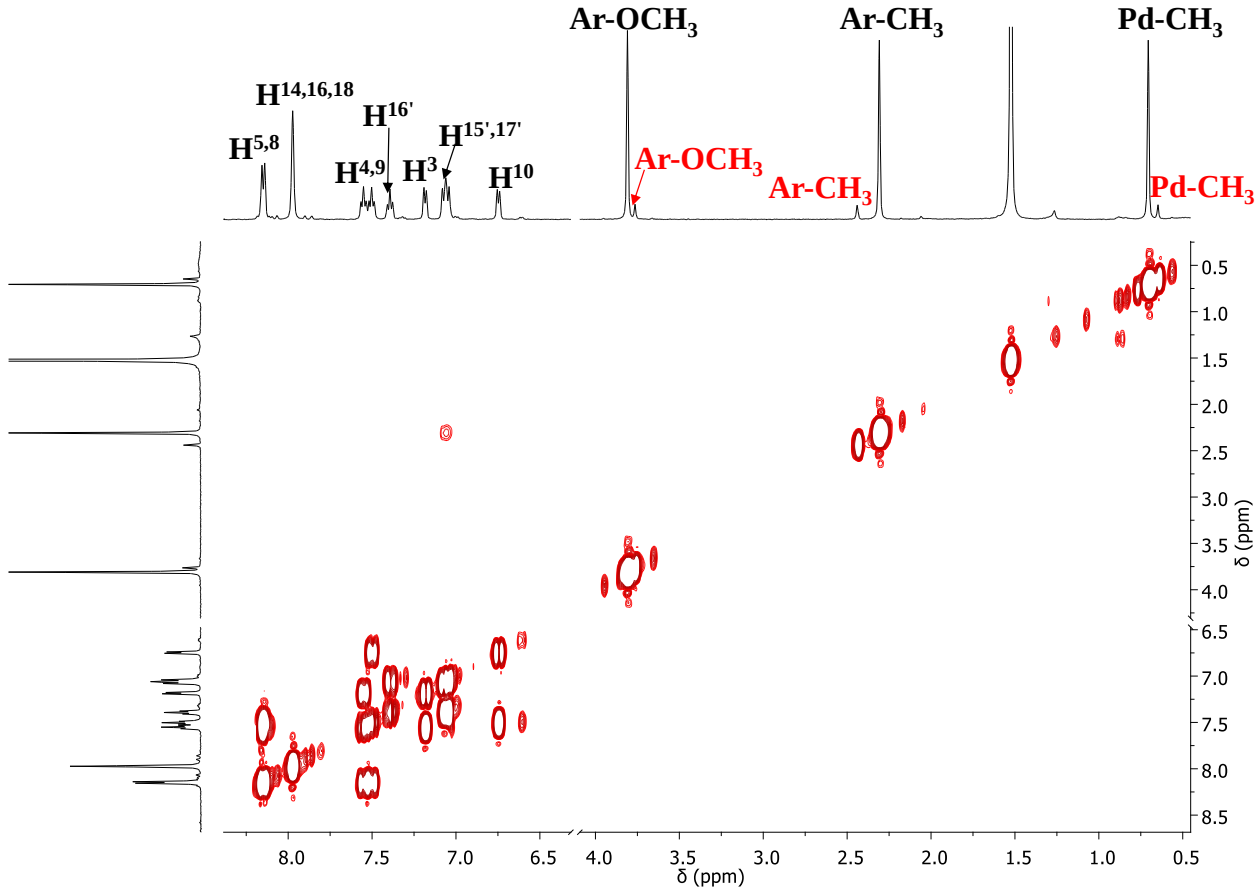

Figure S11. {^{1}H,^{1}H}-COSY spectrum of complex **1a** in CD_2Cl_2 at 298 K. *trans* (black) and *cis* (red) isomers.

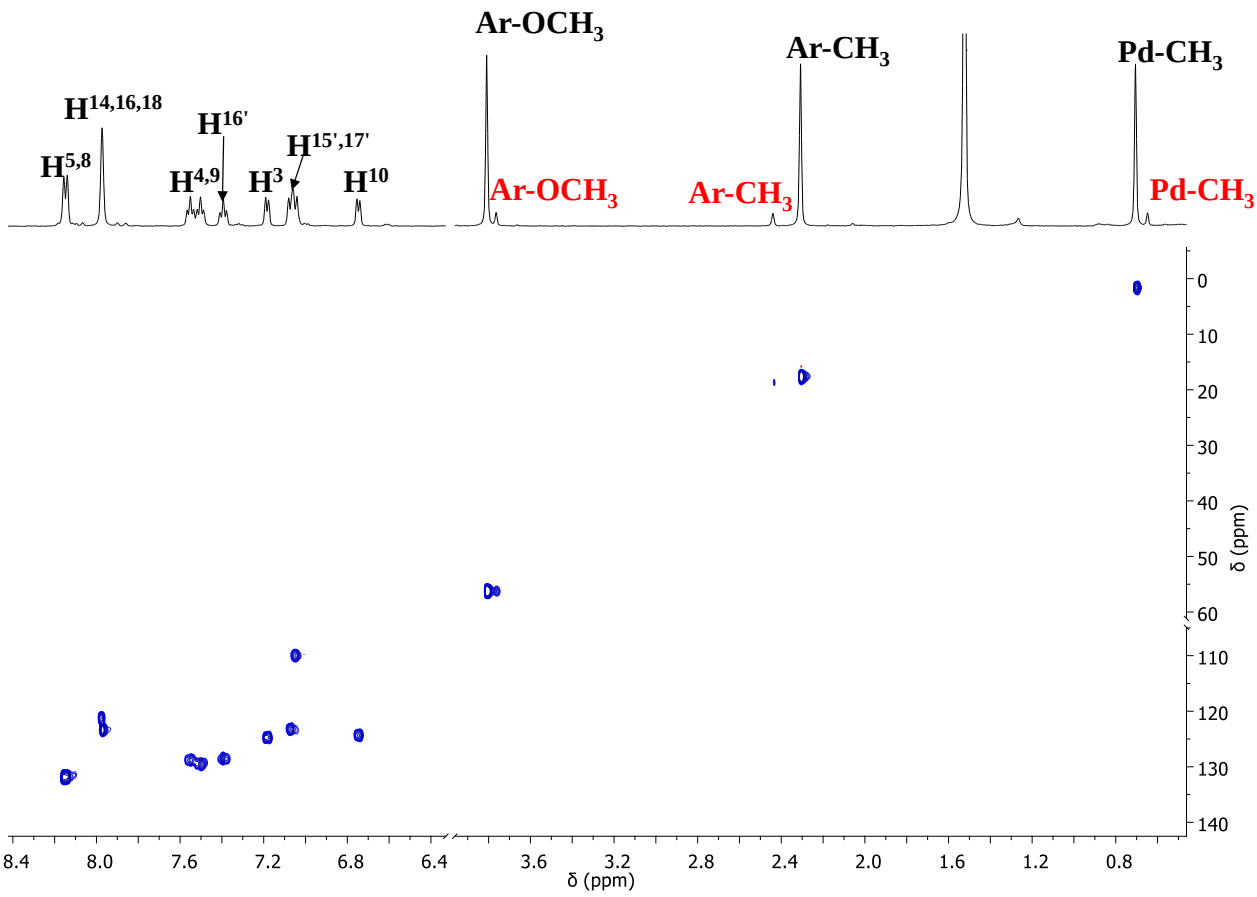

Figure S12. {^{1}H,^{13}C}-HSQC spectrum of complex **1a** in CD_2Cl_2 at 298 K. *trans* (black) and *cis* (red) isomers.

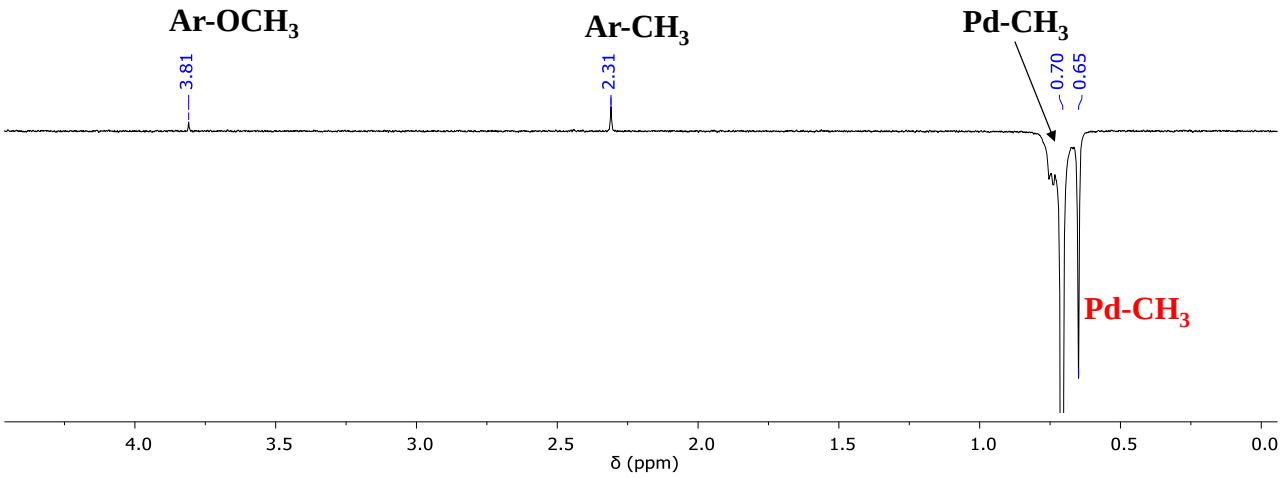

Figure S13. 1D-NOESY spectrum of complex **1a** in CD_2Cl_2 at 298 K obtained by irradiating the most intense Pd-CH_3 signal. Aliphatic region. *trans* (black) and *cis* (red) isomers.

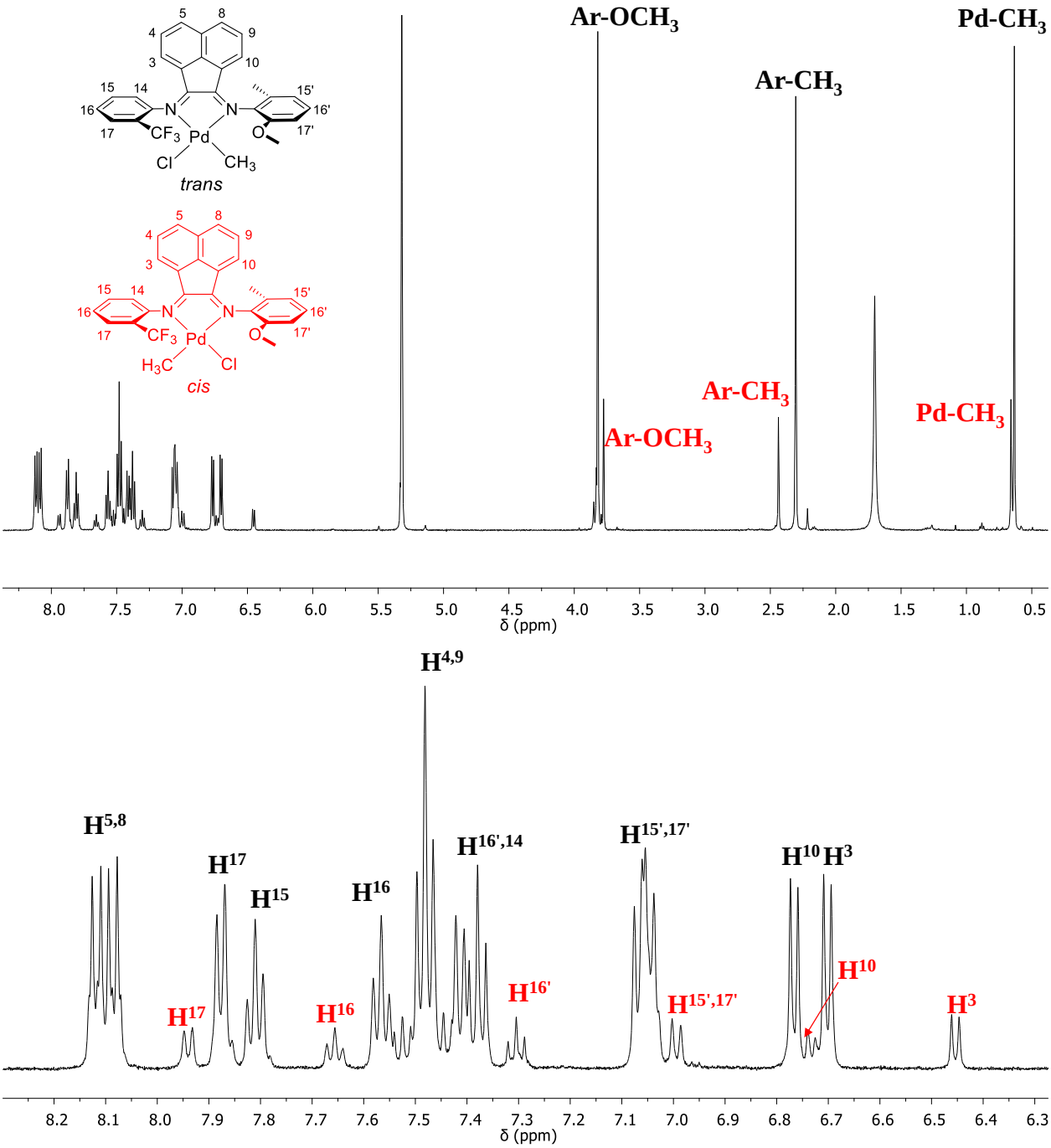

Figure S14. ^{1}H NMR spectrum of complex **2a** in CD_2Cl_2 at 298 K (top); enlargement of the aromatic region (bottom). *trans* (black) and *cis* (red) isomers.

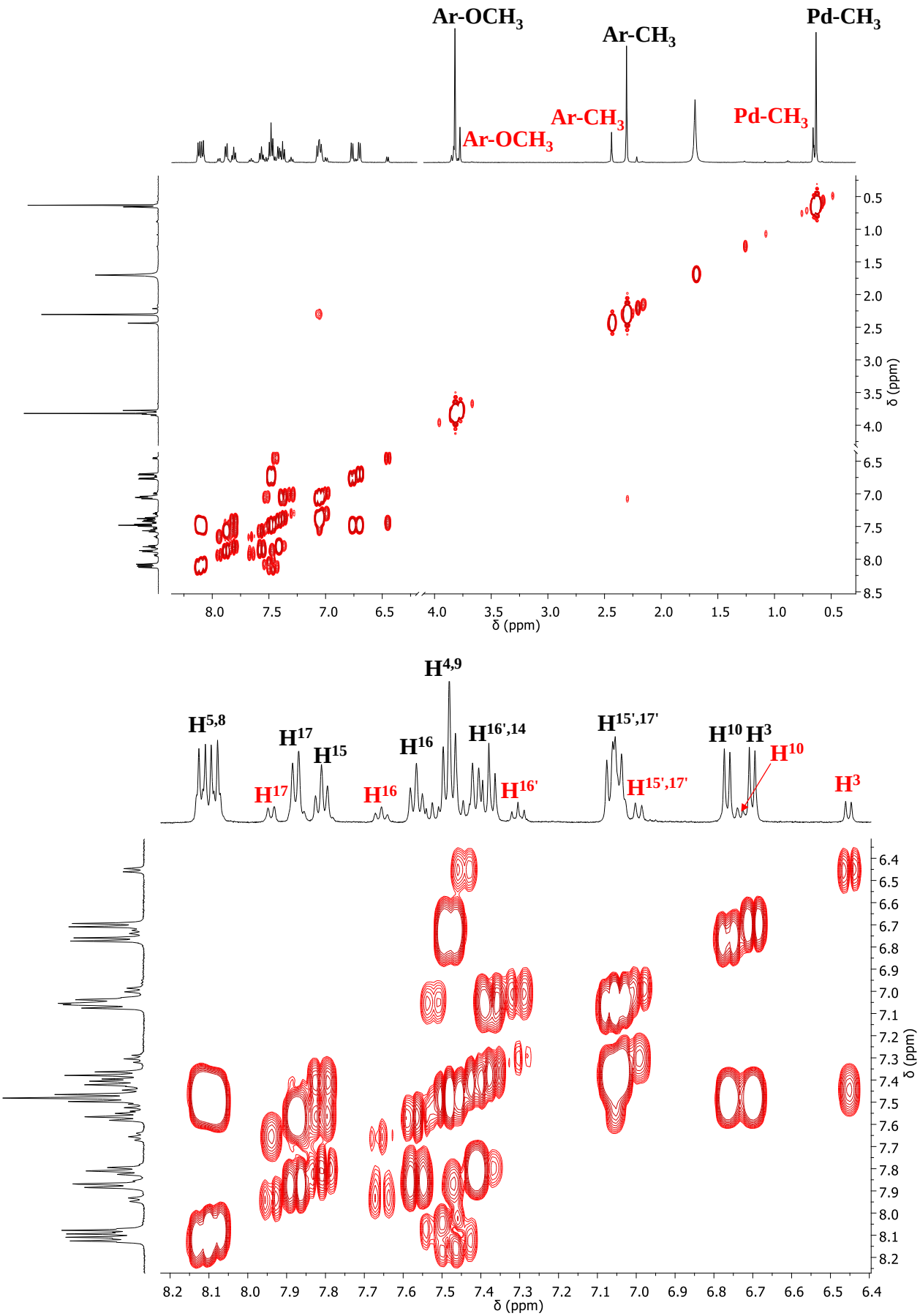

Figure S15. {^{1}H,^{1}H}-COSY spectrum of complex **2a** in CD_2Cl_2 at 298 K (top); enlargement of the aromatic region (bottom). *trans* (black) and *cis* (red) isomers.

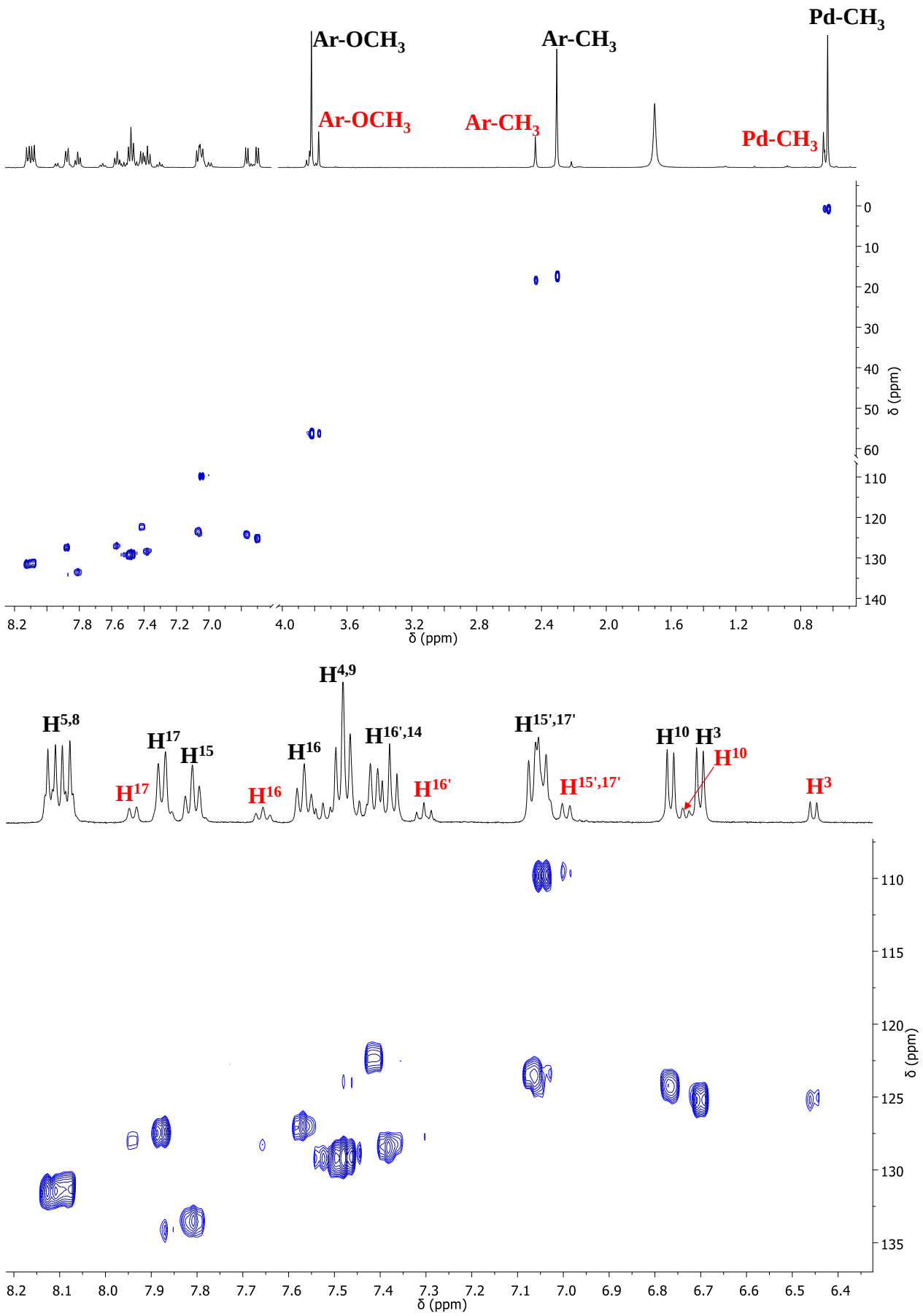

Figure S16. {^{1}H,^{13}C}-HSQC spectrum of complex **2a** in CD_2Cl_2 at 298 K (top); enlargement of the aromatic region (bottom). *trans* (black) and *cis* (red) isomers.

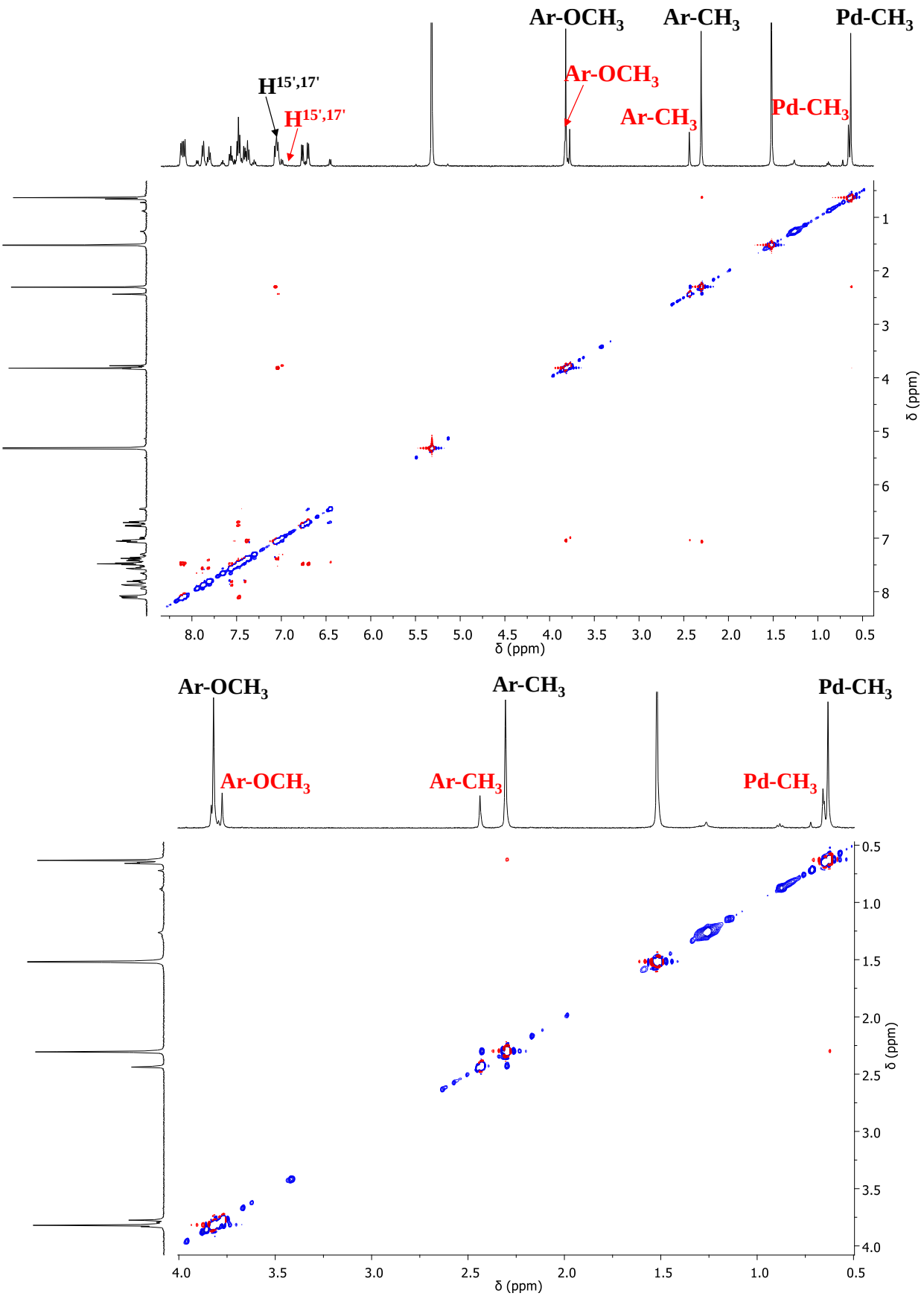

Figure S17. {^{1}H,^{1}H}-NOESY spectrum of complex **2a** in CD_2Cl_2 at 298 K (top); enlargement of the aliphatic region (bottom). *trans* (black) and *cis* (red) isomers. Red peaks are due to NOE, blue peaks are due to exchange.

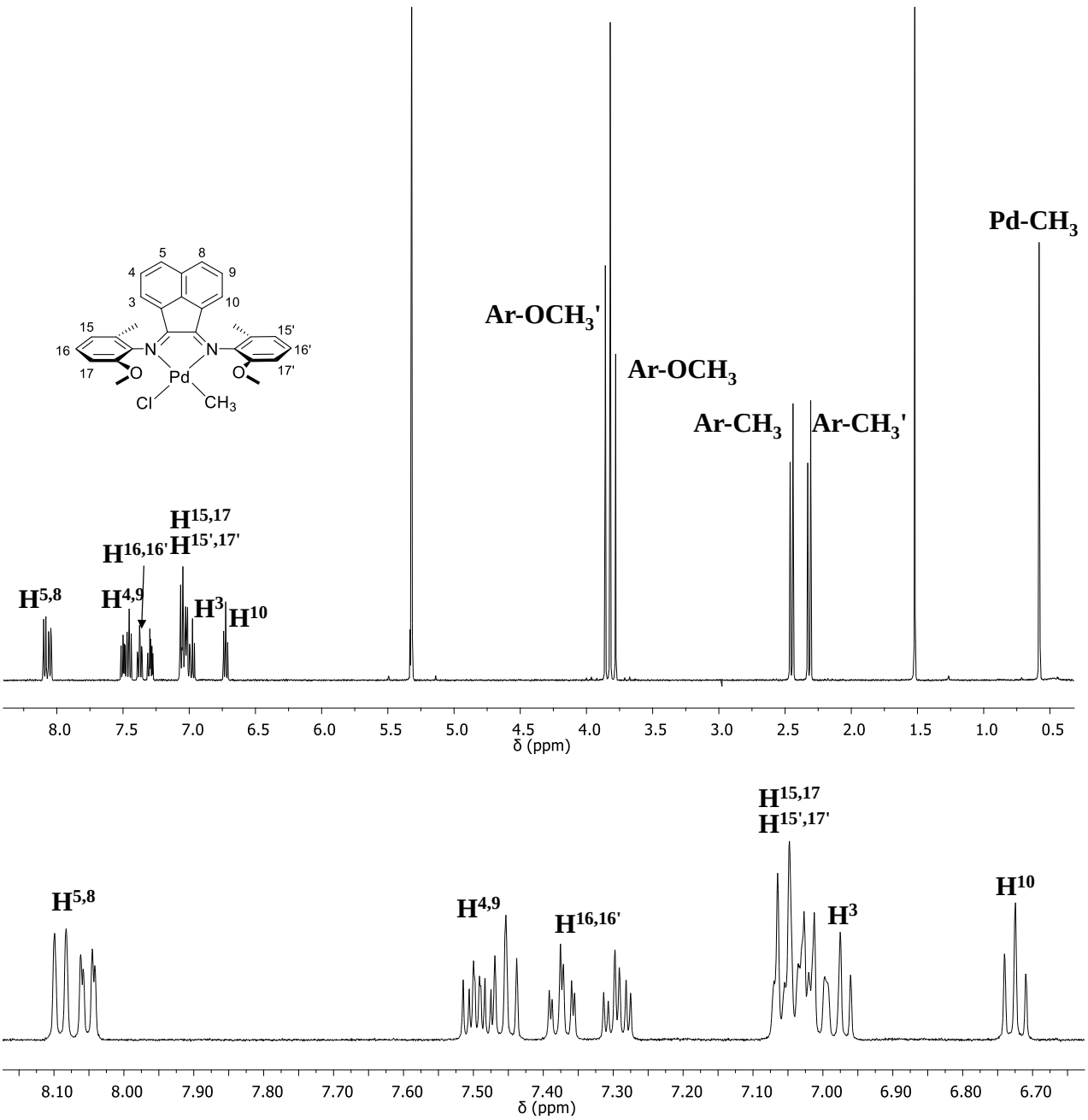

Figure S18. ^{1}H NMR spectrum of complex **3a** in CD_2Cl_2 at 298 K (top); enlargement of the aromatic region (bottom).

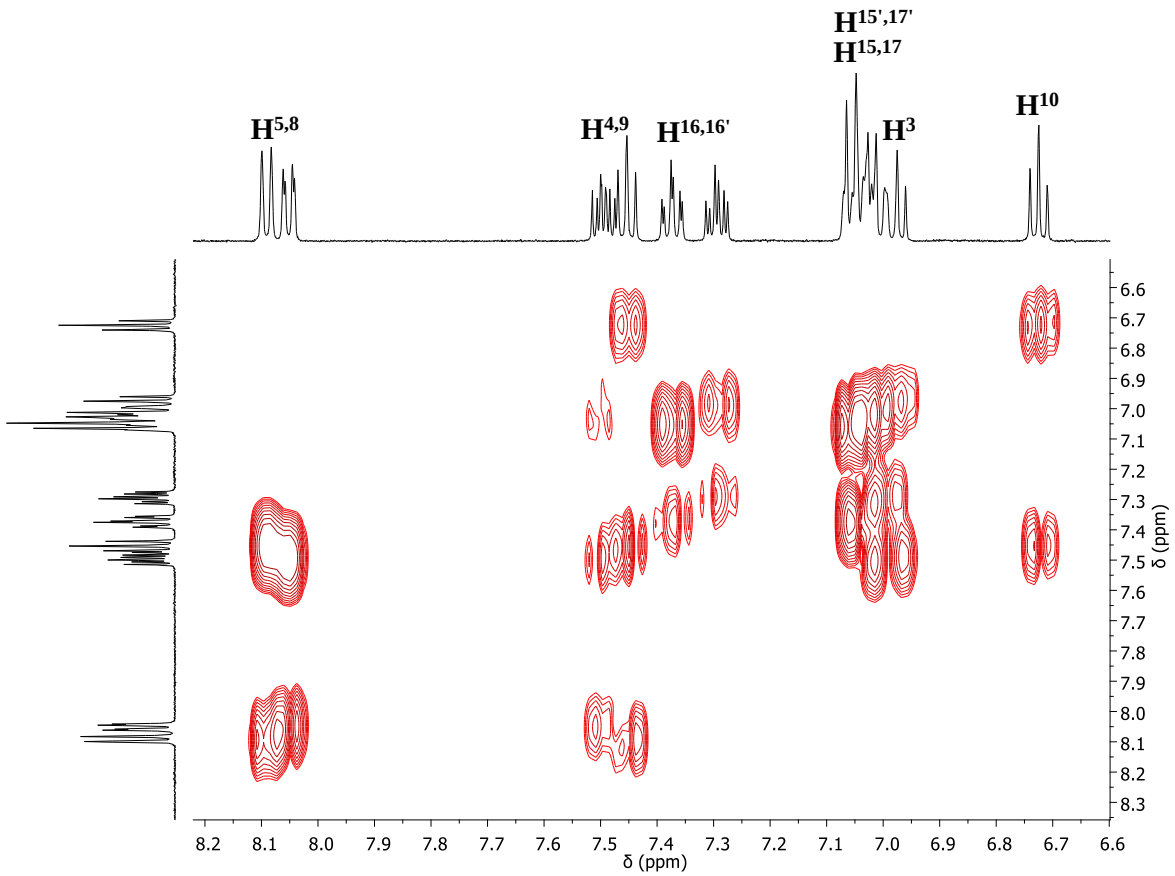

Figure S19. {^{1}H,^{1}H}-COSY spectrum of complex **3a** in CD_2Cl_2 at 298 K; enlargement of the aromatic region.

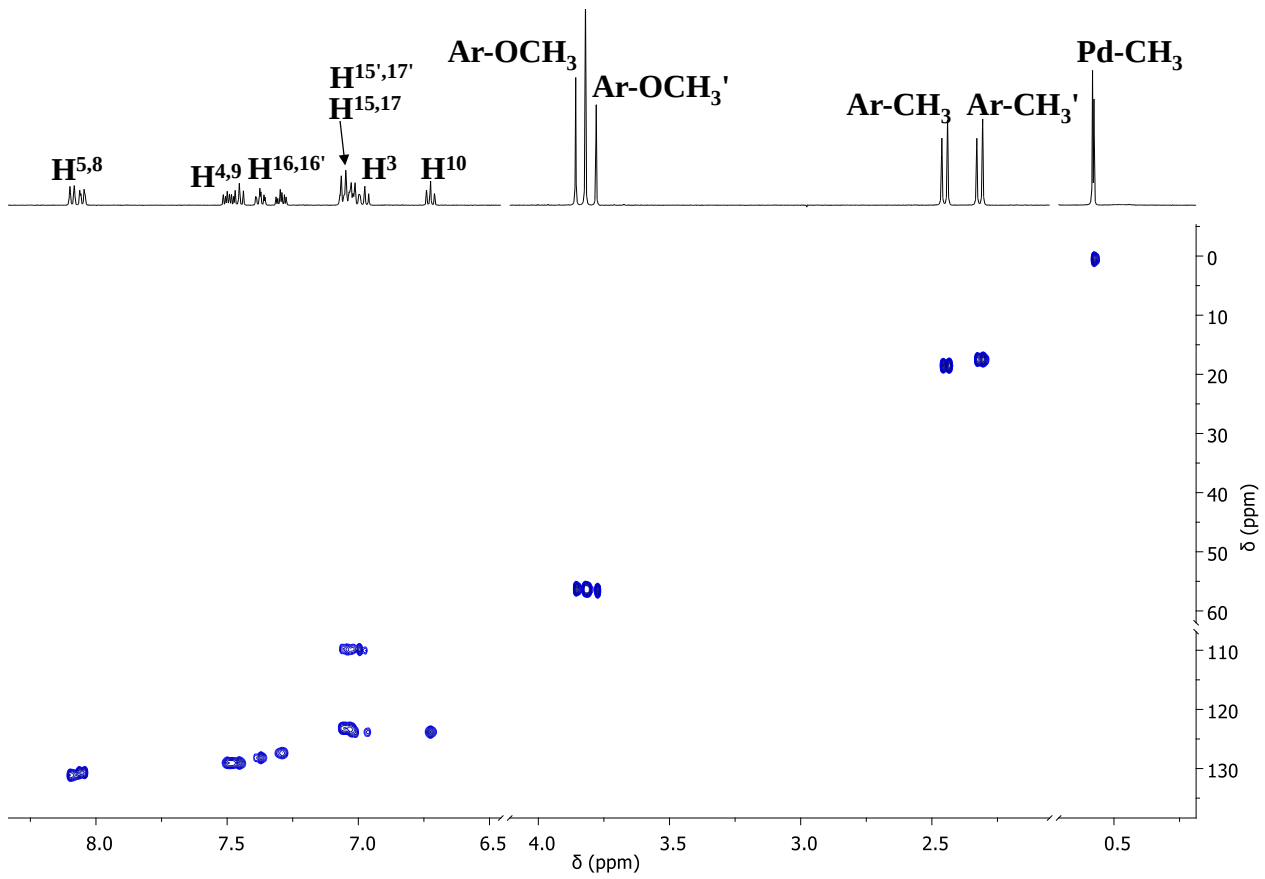

Figure S20. {^{1}H,^{13}C}-HSQC spectrum of complex **3a** in CD_2Cl_2 at 298 K.

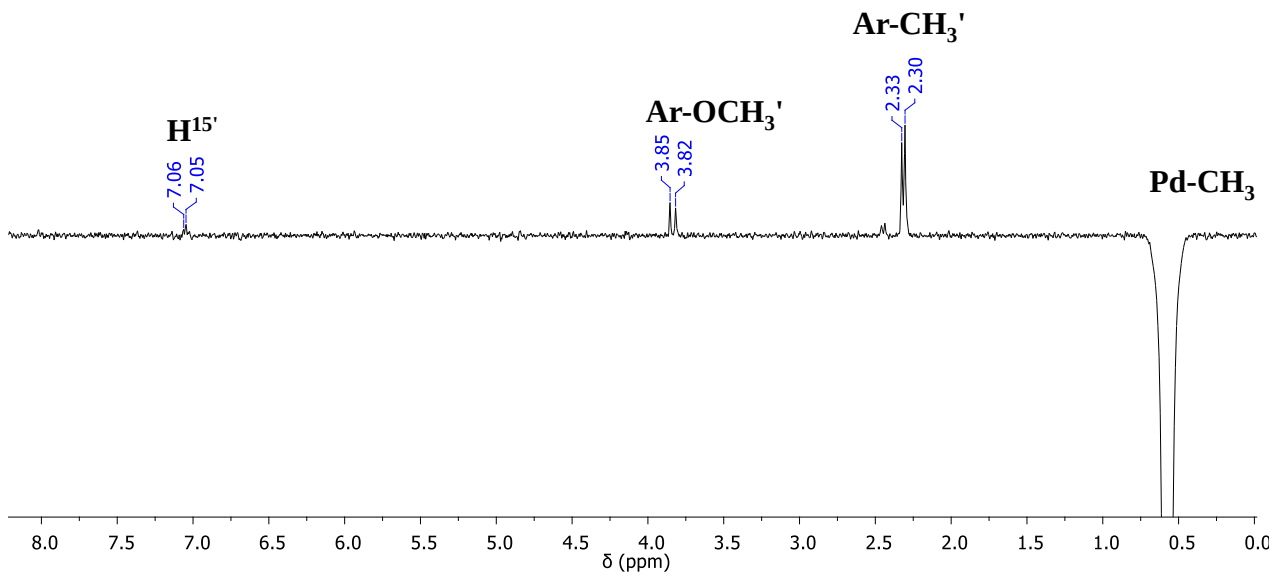

Figure S21. 1D-NOESY spectrum of complex **3a** in CD_2Cl_2 at 298 K obtained by irradiating the Pd-CH_3 signal.

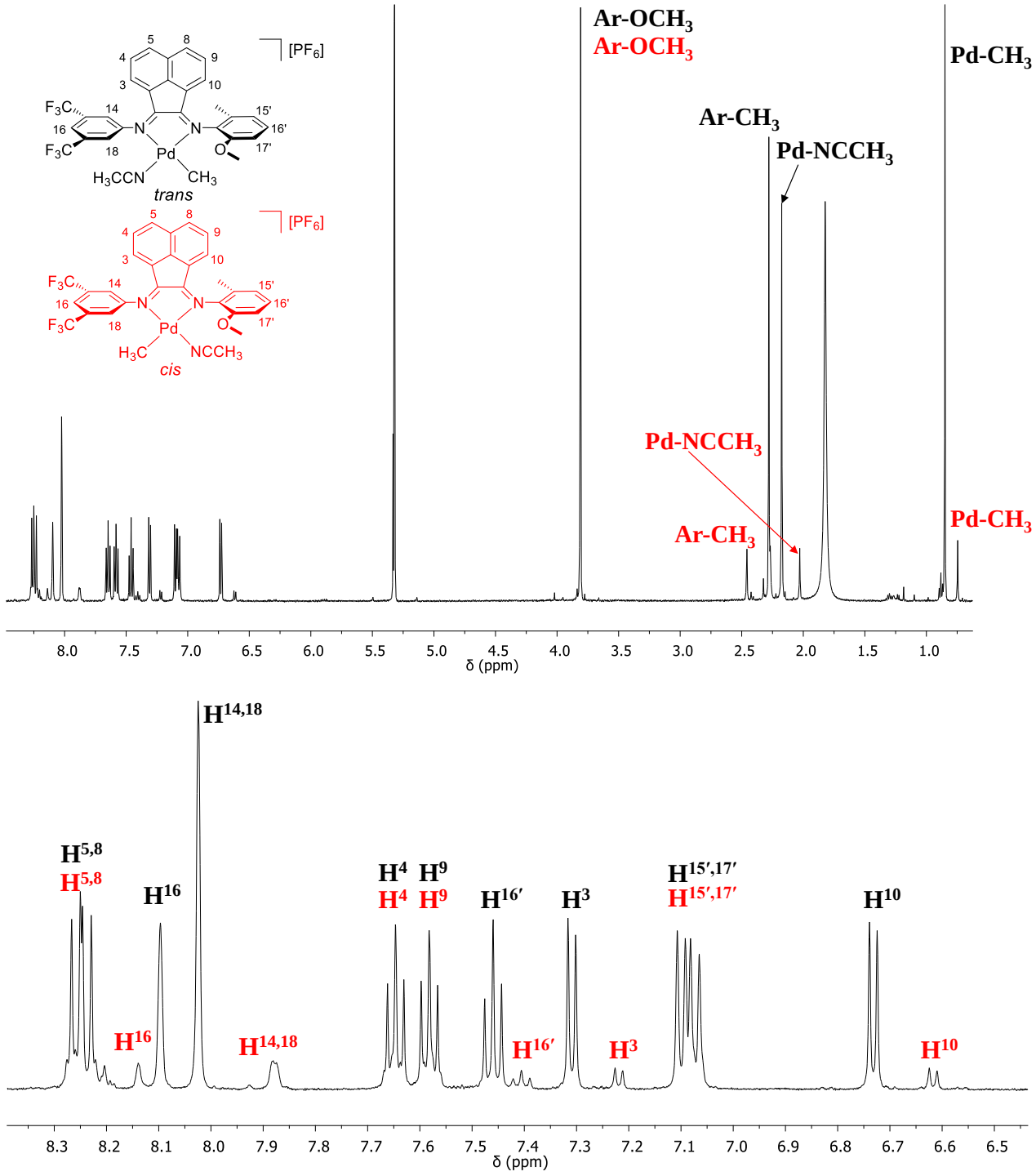

Figure S22. ^{1}H NMR spectrum of complex **1b** in CD_2Cl_2 at 298 K (top); enlargement of the aromatic region (bottom). *trans* (black) and *cis* (red) isomers.

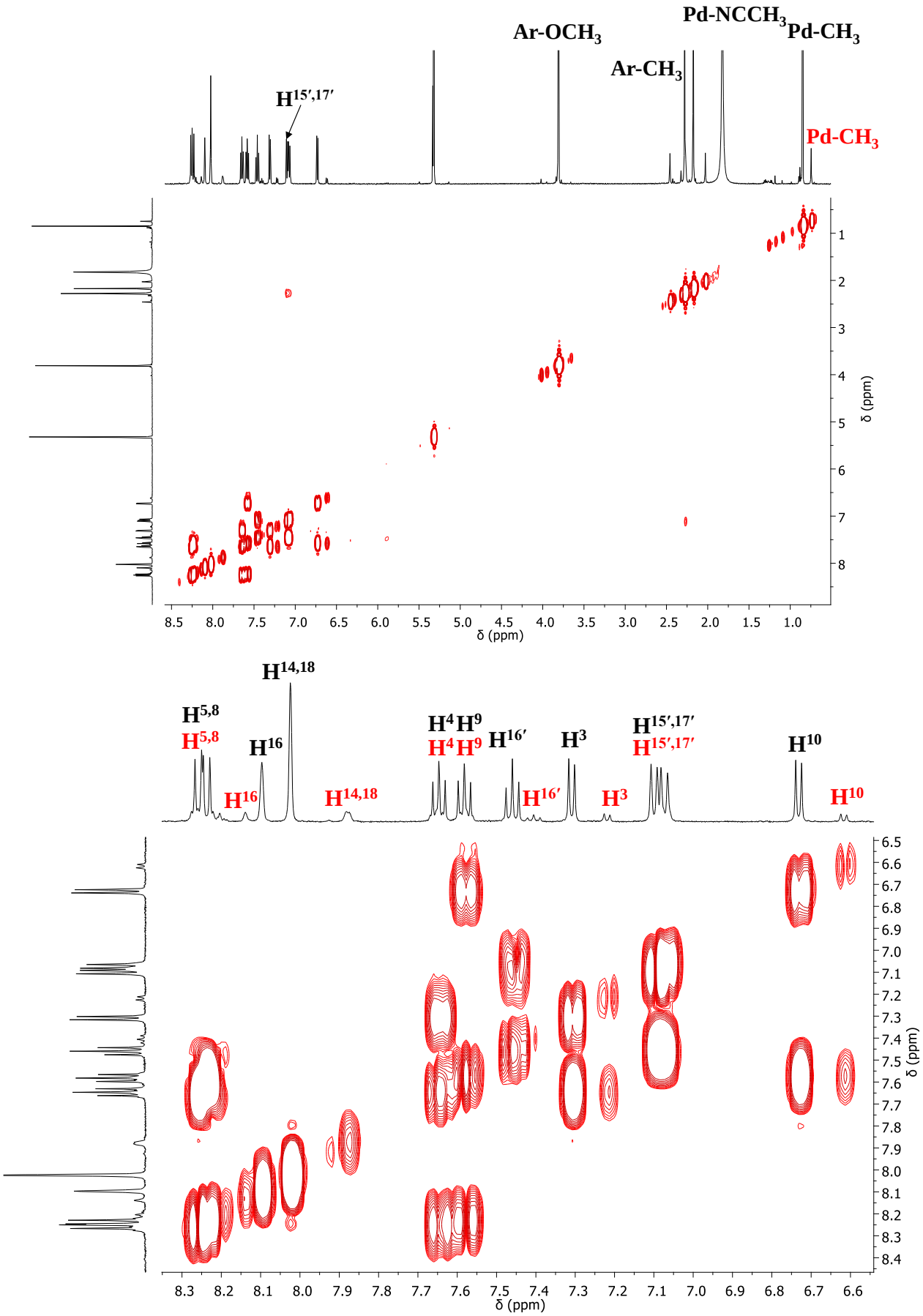

Figure S23. {^{1}H,^{1}H}-COSY spectrum of complex **1b** in CD_2Cl_2 at 298 K (top); enlargement of the aromatic region (bottom). *trans* (black) and *cis* (red) isomers.

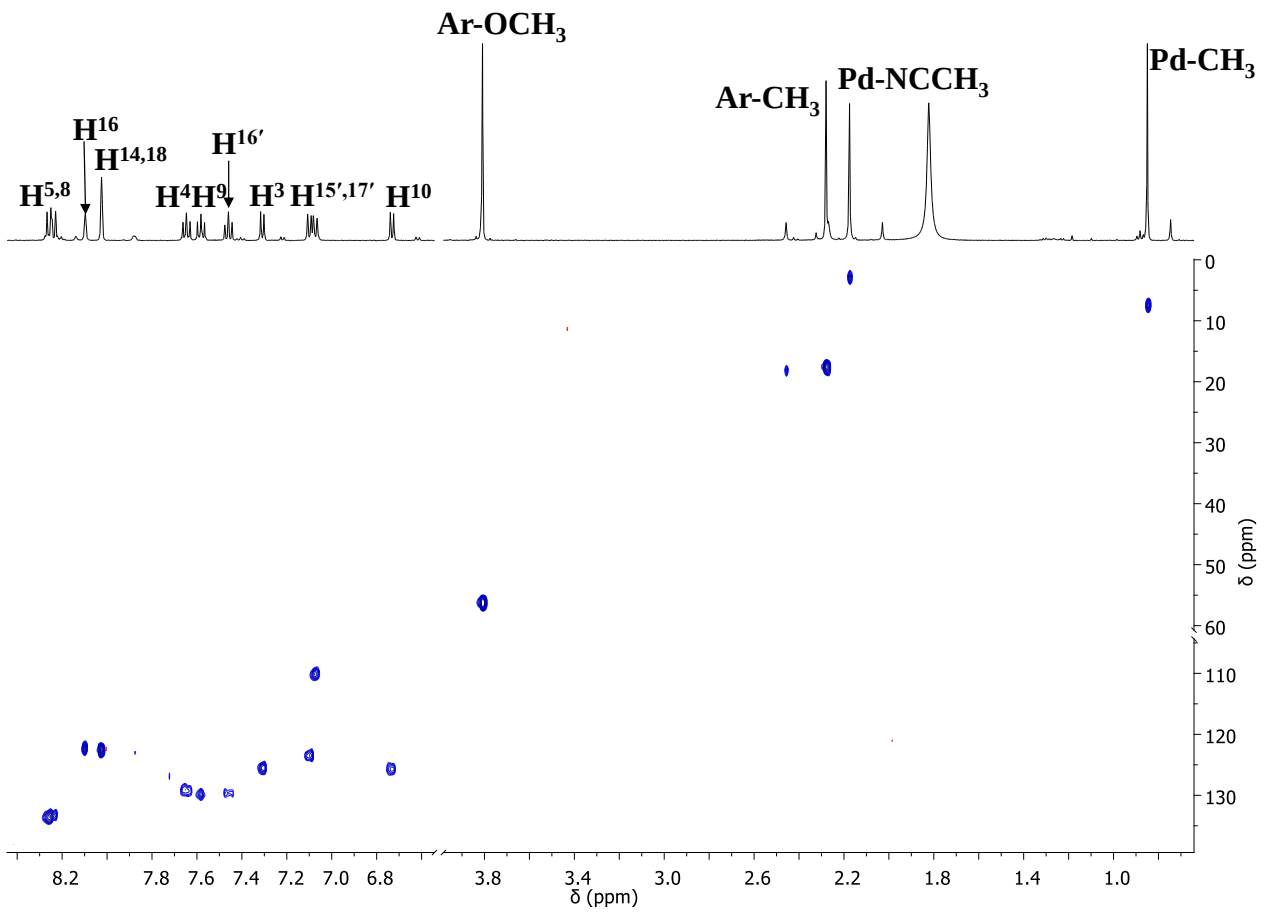

Figure S24. **{**^{1}H,^{13}C}-HSQC spectrum of complex **1b** in CD_2Cl_2 at 298 K. Only the *trans* isomer is labeled.

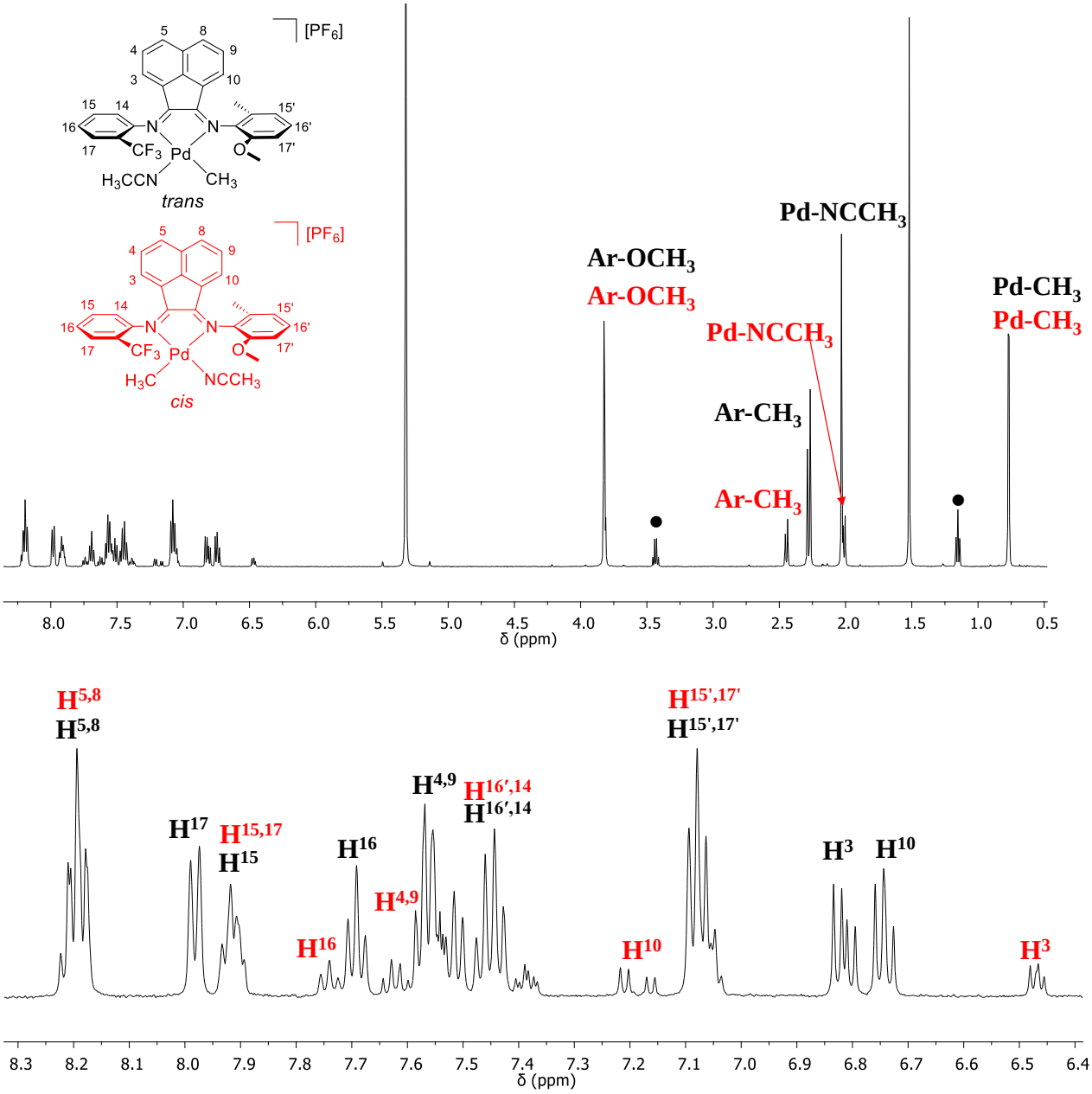

Figure S25. ^{1}H NMR spectrum of complex **2b** in CD_2Cl_2 at 298 K (top); enlargement of the aromatic region (bottom). *trans* (black) and *cis* (red) isomers. ● diethyl ether.

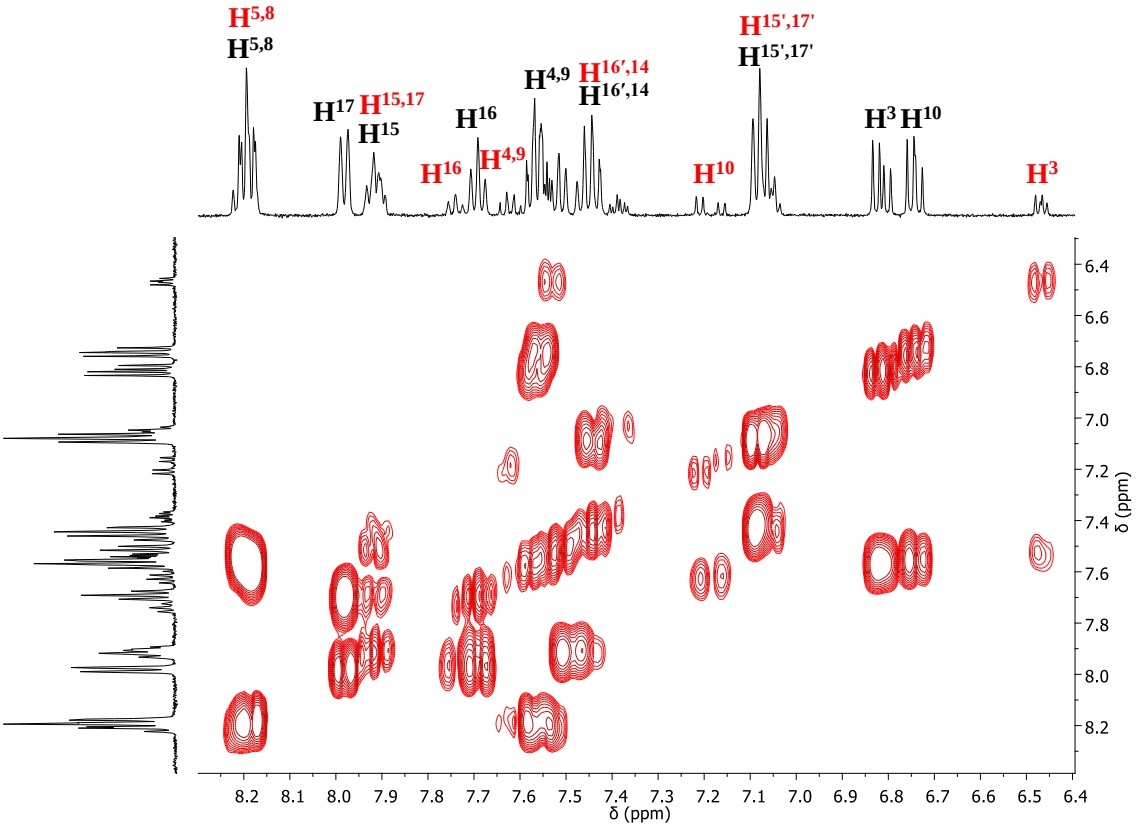

Figure S26. {^{1}H,^{1}H}-COSY spectrum of complex **2b** in CD_2Cl_2 at 298 K. Aromatic region. *trans* (black) and *cis* (red) isomers.

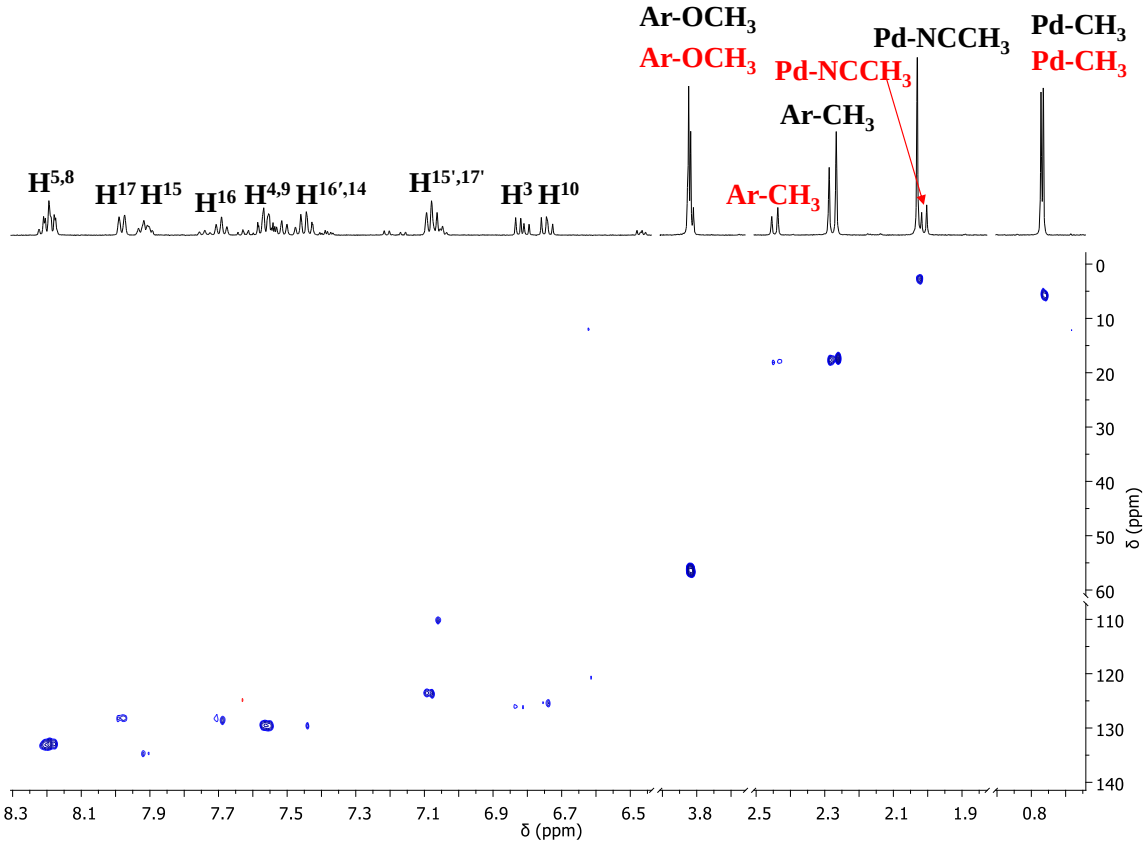

Figure S27. {^{1}H,^{13}C}-HSQC spectrum of complex **2b** in CD_2Cl_2 at 298 K. *trans* (black) and *cis* (red) isomers.

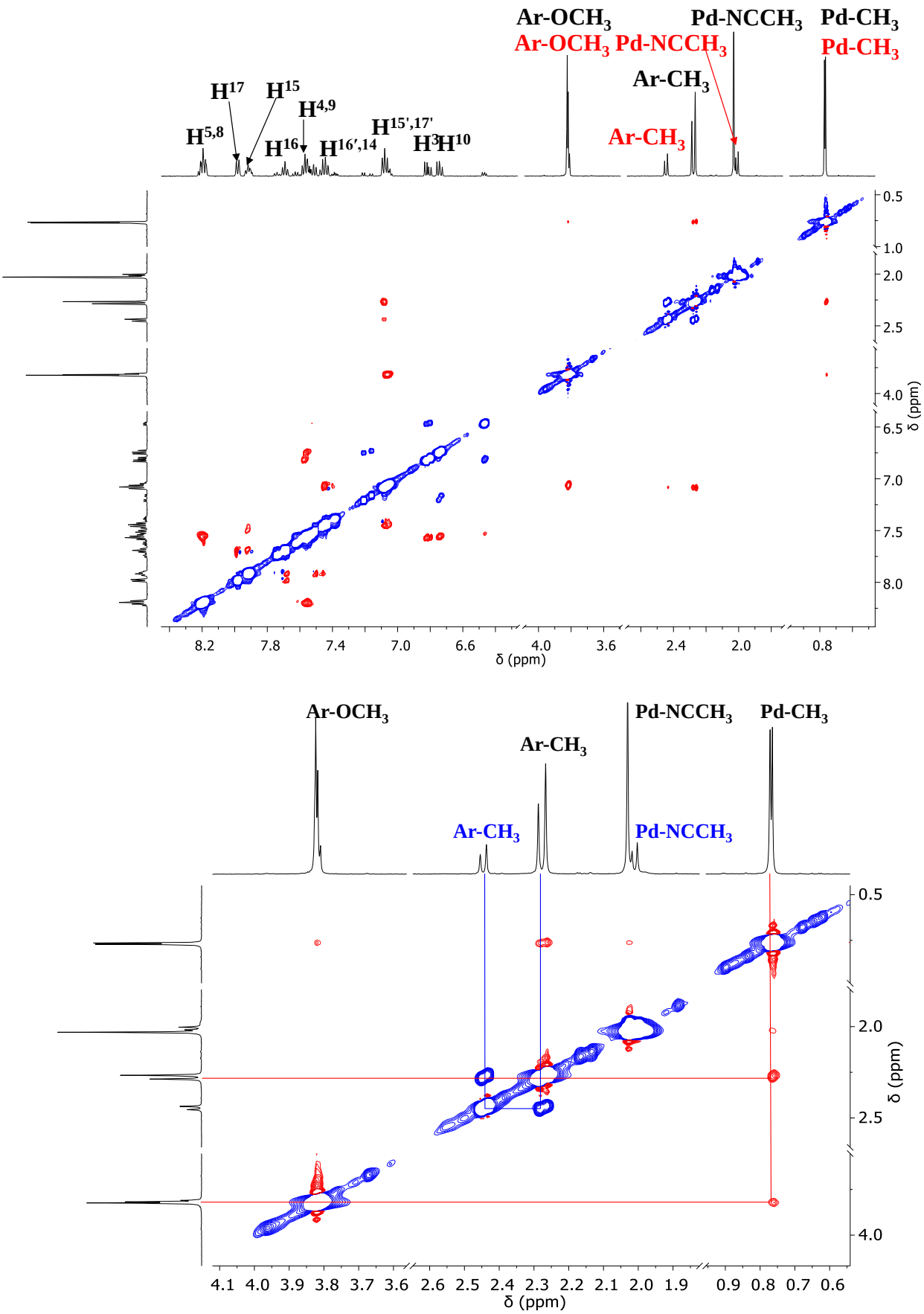

Figure S28. {^{1}H,^{1}H}-NOESY spectrum of complex **2b** in CD_2Cl_2 at 298 K K (top); enlargement of the aliphatic region (bottom); *trans* (black) and *cis* (red) isomers. Red peaks are due to NOE, blue peaks are due to exchange.

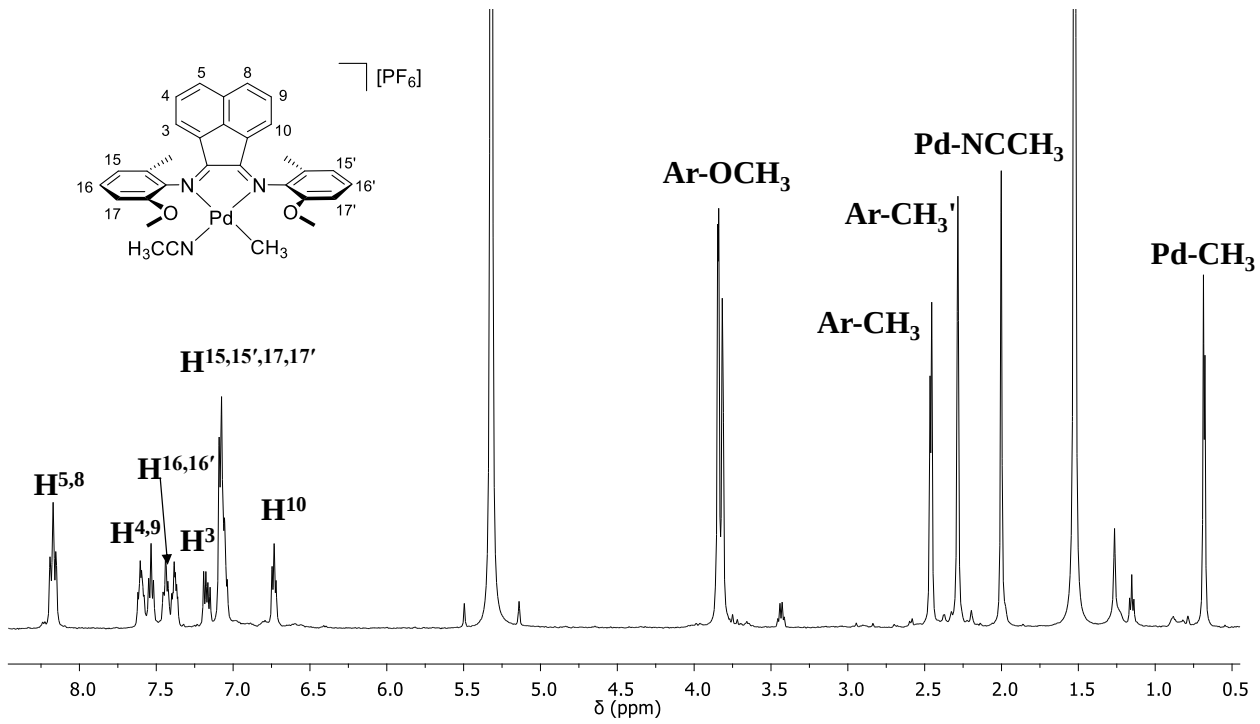

Figure S29. ^{1}H NMR spectrum of complex **3b** in CD_2Cl_2 at 298 K. *trans* (black) and *cis* (red) isomers.

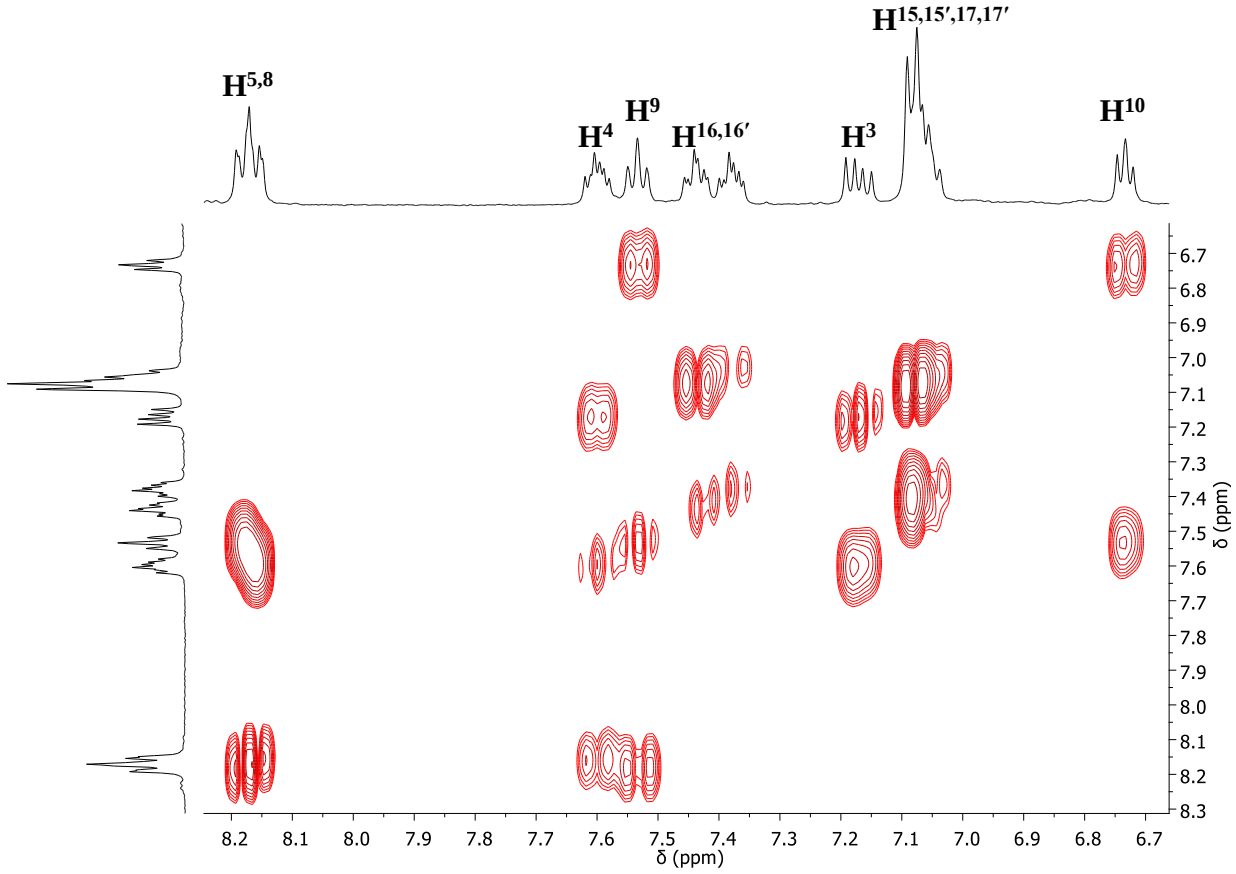

Figure S30. {^{1}H,^{1}H}-COSY spectrum of complex **3b** in CD_2Cl_2 at 298 K. Aromatic region.

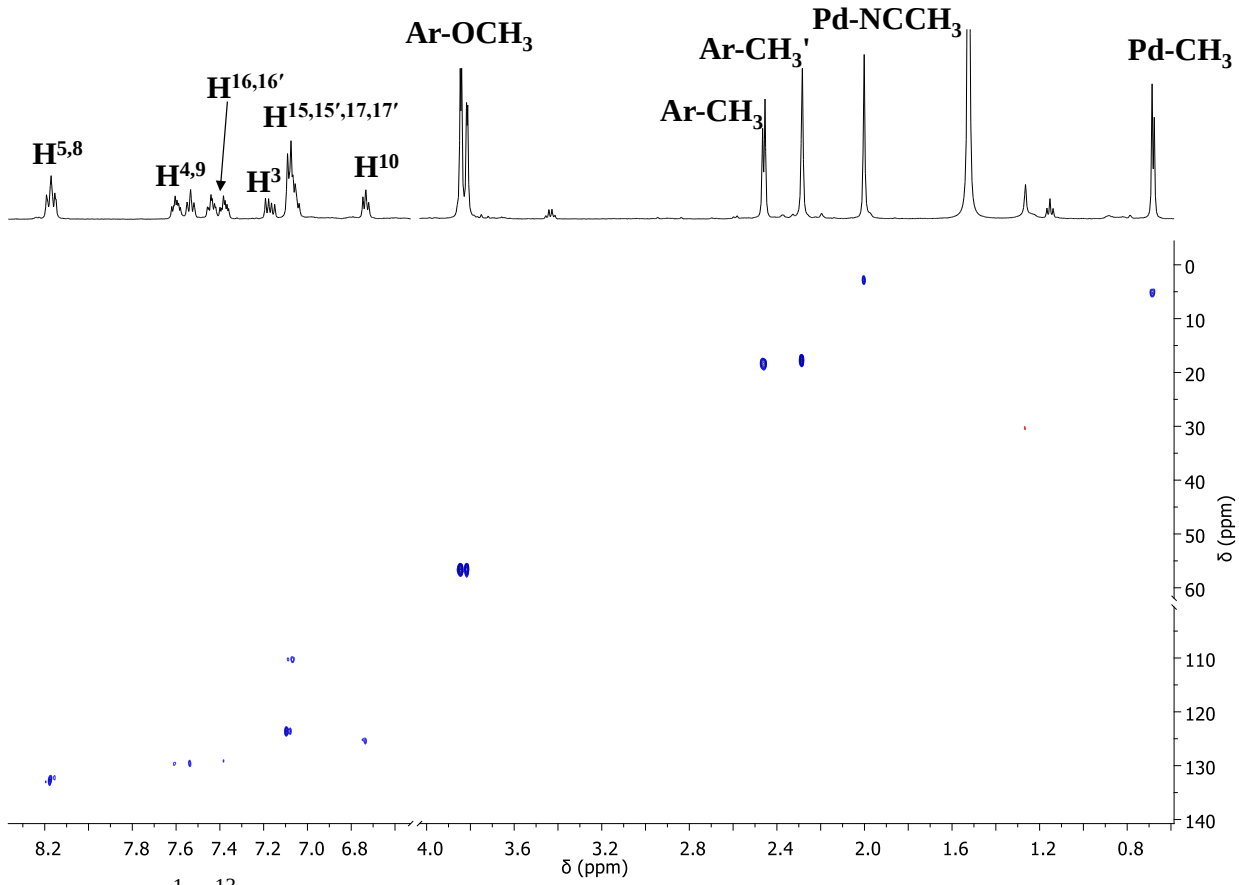

Figure S31. {^{1}H,^{13}C}-HSQC spectrum of complex **3b** in CD_2Cl_2 at 298 K.

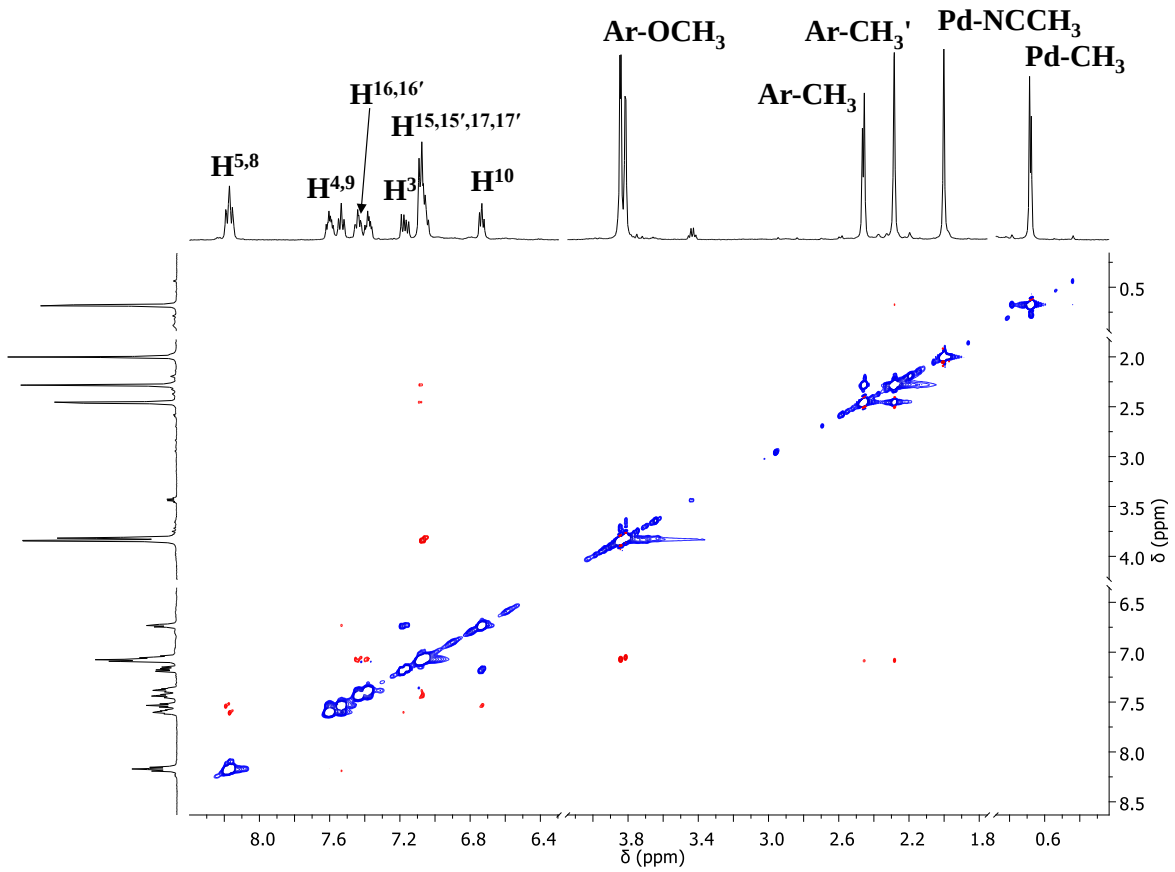

Figure S32. {^{1}H,^{1}H}-NOESY spectrum of complex **3b** in CD_2Cl_2 at 298 K. Red peaks are due to NOE, blue peaks are due to exchange.

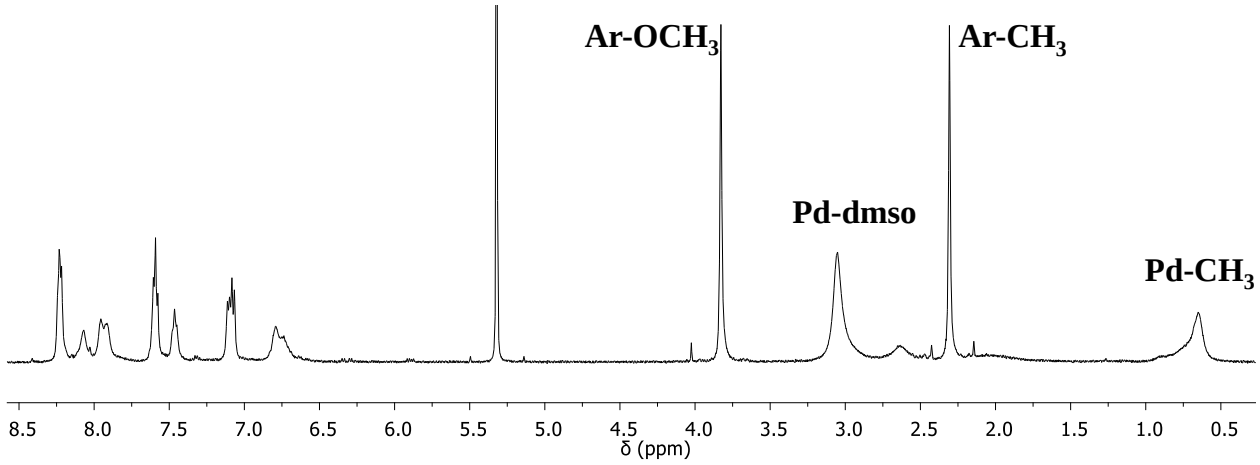

Figure S33. ^{1}H NMR spectrum of complex **1c** in CD_2Cl_2 at 298 K.

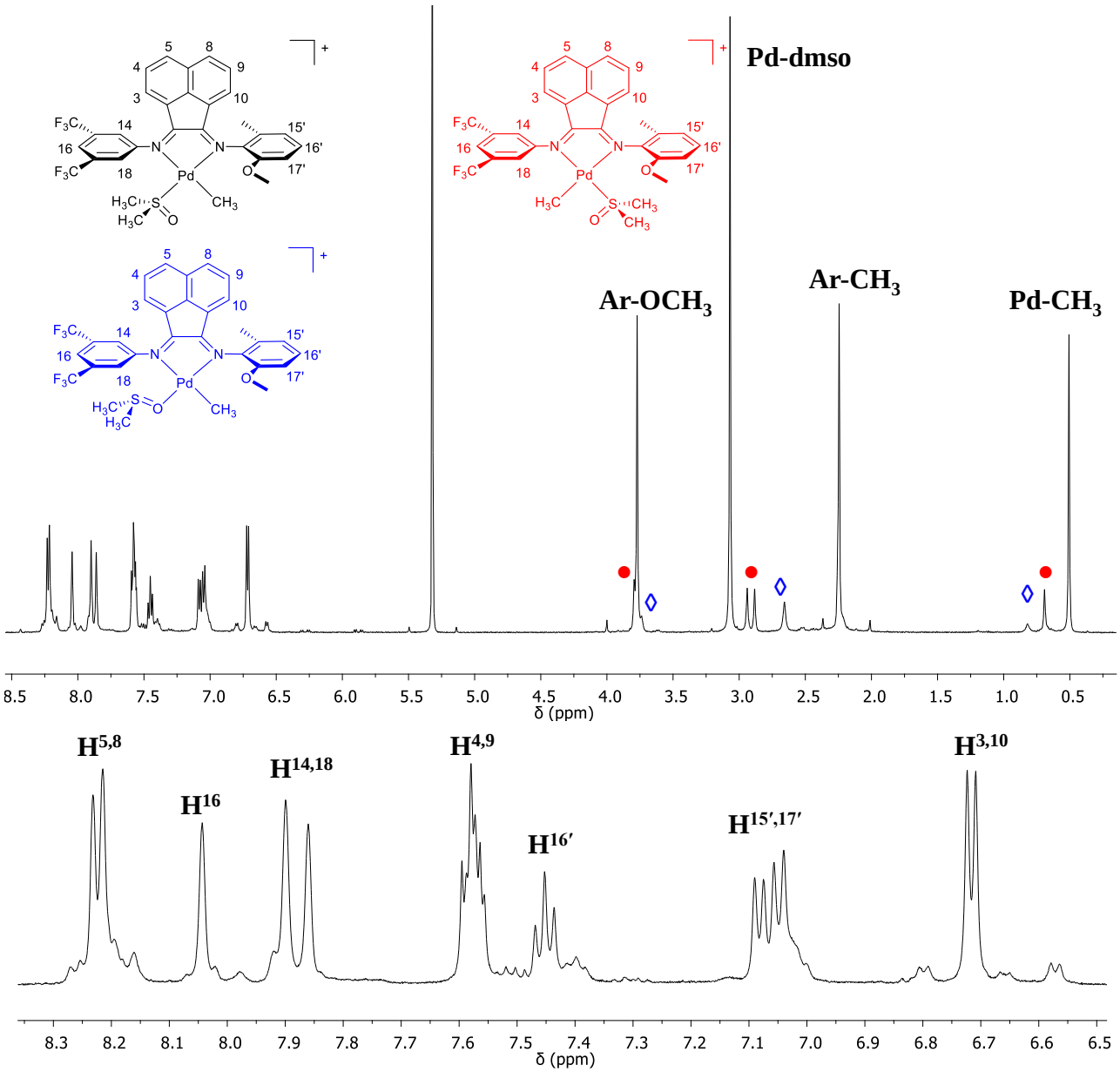

Figure S34. ^{1}H NMR spectrum of complex **1c** in CD_2Cl_2 at 233 K (top); enlargement of the aromatic region (bottom). S-bonded dmso *trans* isomer (black), *cis* isomer (●); O-bonded dmso *trans* isomer (◊).

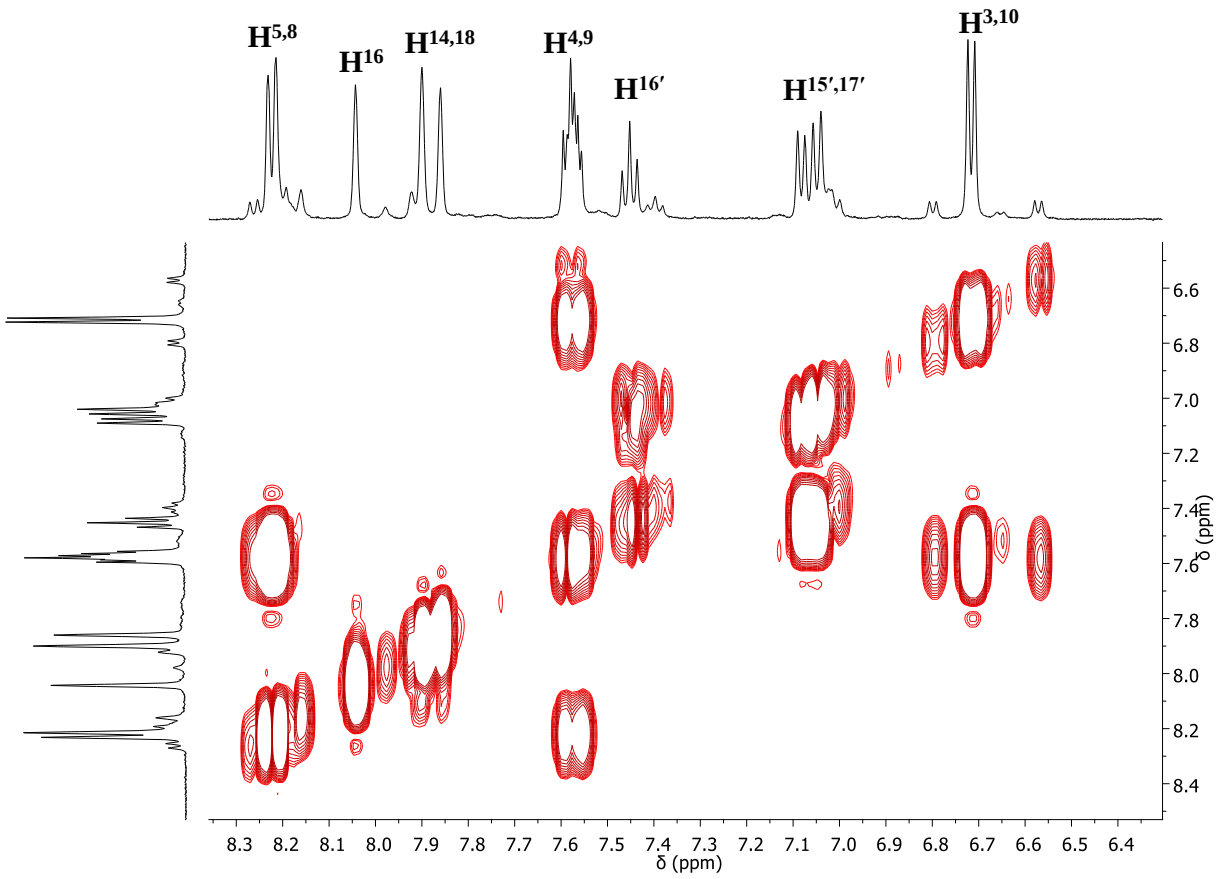

Figure S35. {^{1}H,^{1}H}-COSY spectrum of complex **1c** in CD_2Cl_2 at 233 K. Aromatic region.

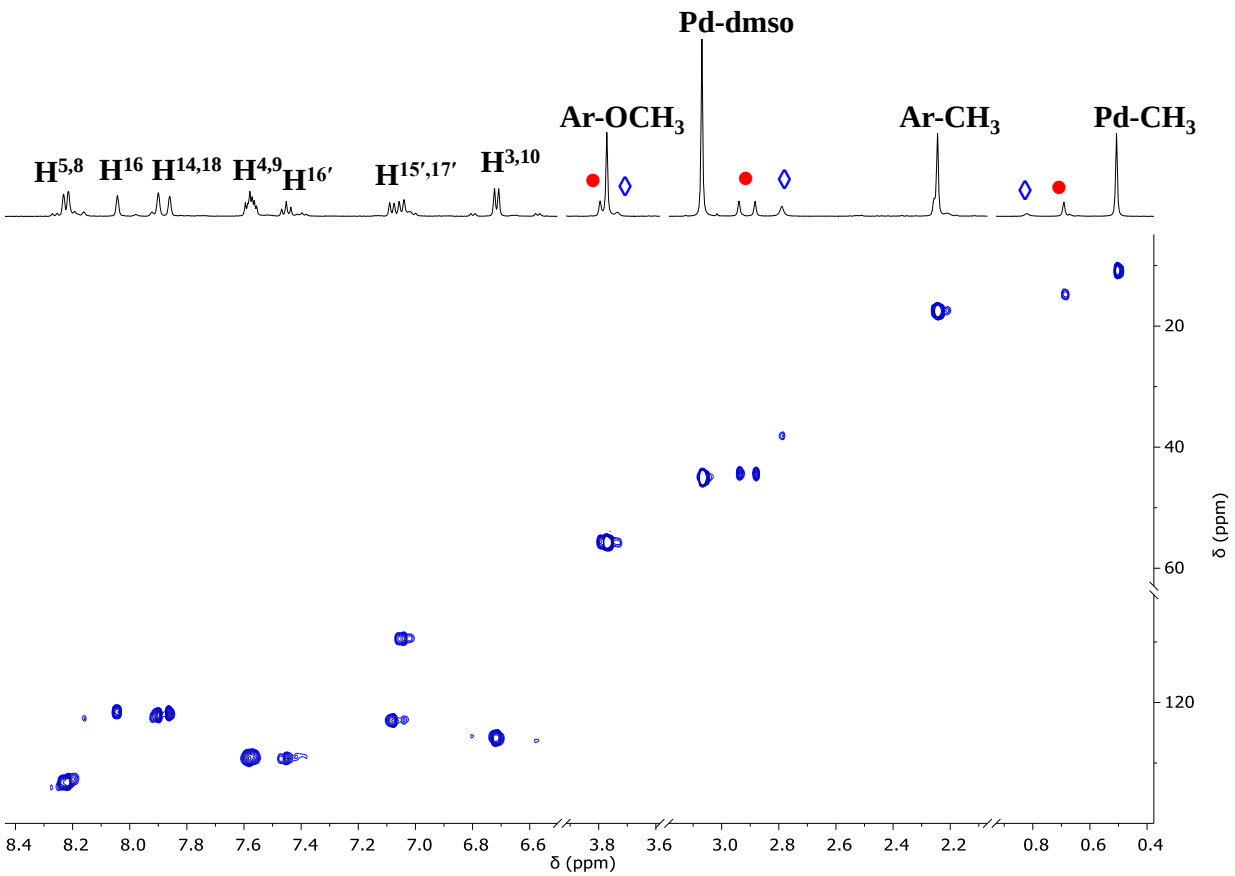

Figure S36. **{**^{1}H,^{13}C}-HSQC spectrum of complex **1c** in CD_2Cl_2 at 233 K.

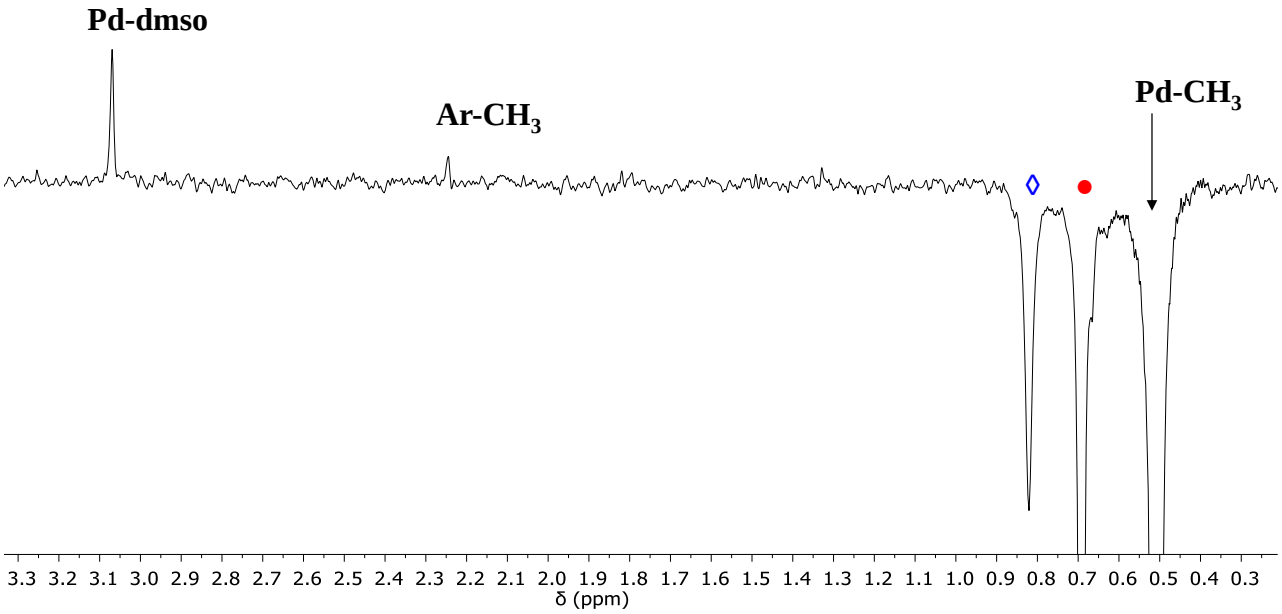

Figure S37. 1D-NOESY spectrum of complex **1c** in CD_2Cl_2 at 233 K obtained by irradiating the Pd-CH_3 signal. S-bonded dmso *trans* isomer (black), *cis* isomer (●); O-bonded dmso *trans* isomer (◊).

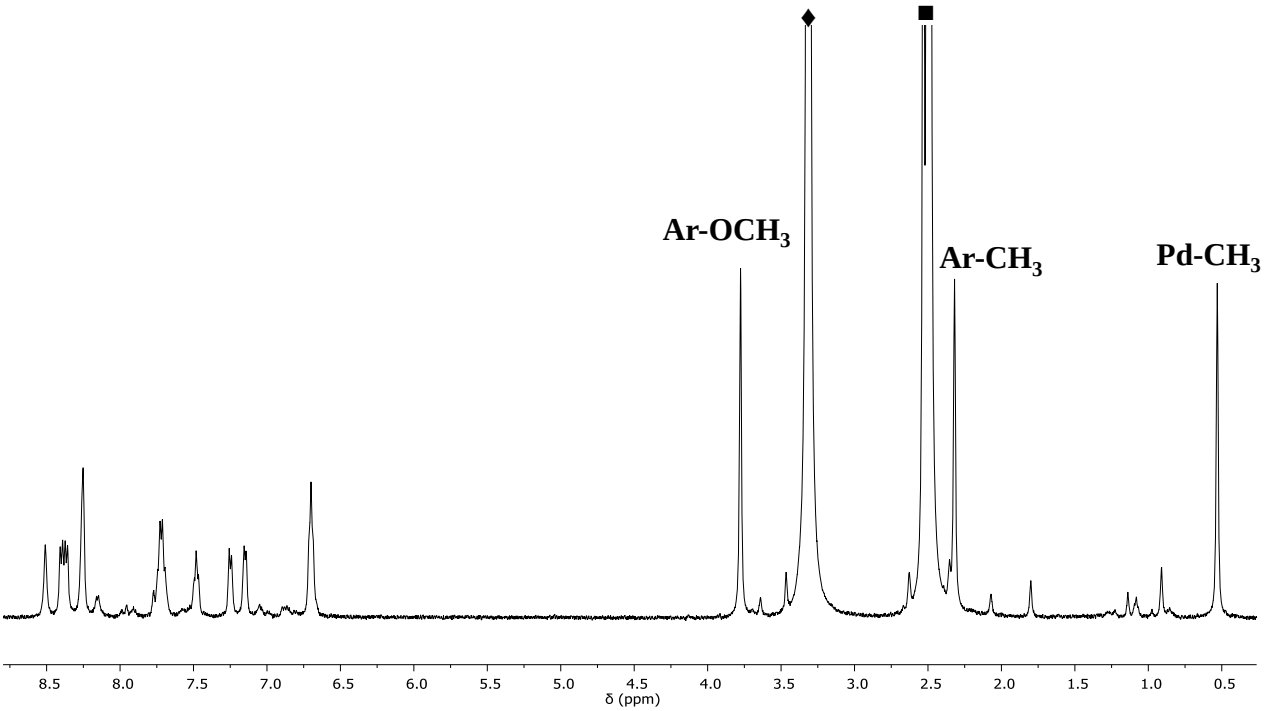

Figure S38. ^{1}H NMR spectrum of complex **1c** in dmso-d_6 at 298 K. ■ free dmso and dmso-d_6; ♦ water.

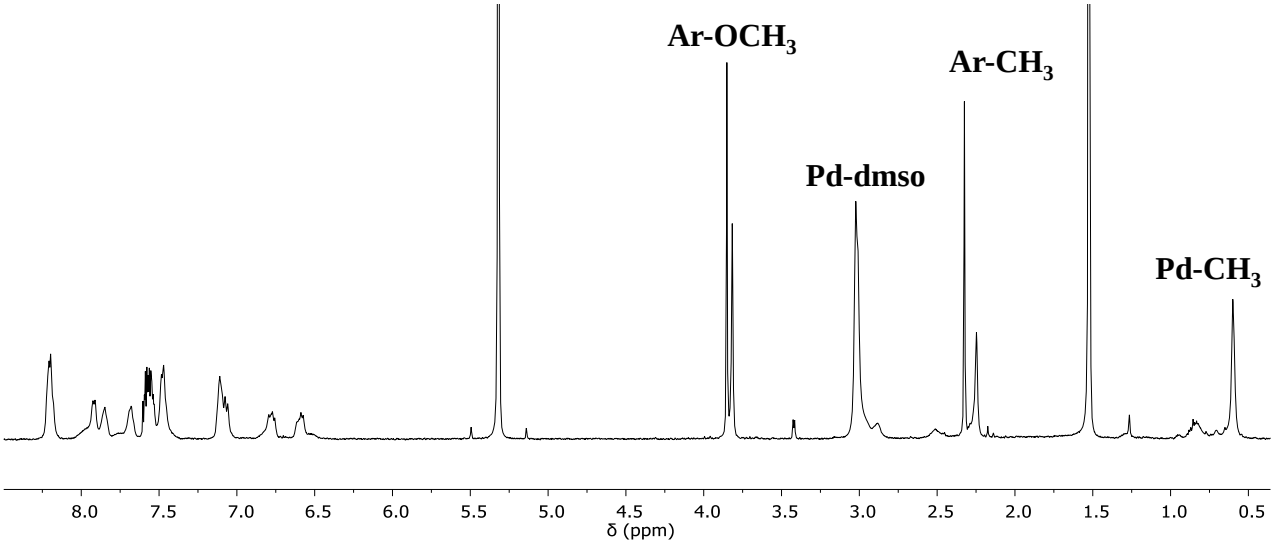

Figure S39. ^{1}H NMR spectrum of complex **2c** in CD_2Cl_2 at 298 K.

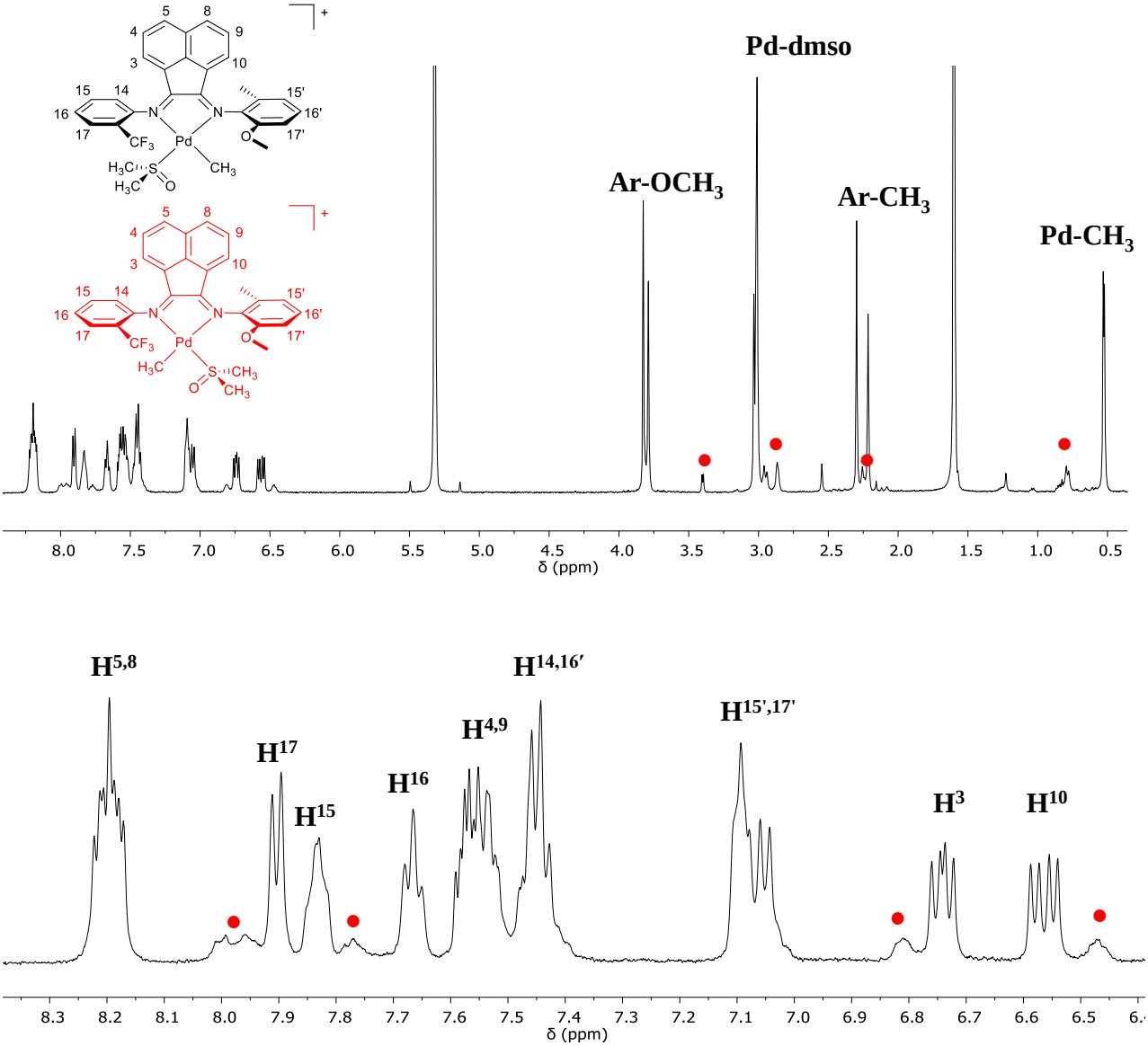

Figure S40. ^{1}H NMR spectrum of complex **2c** in CD_2Cl_2 at 263 K (top); enlargement of the aromatic region (bottom). S-bonded dmso *trans* isomer (black), *cis* isomer (●).

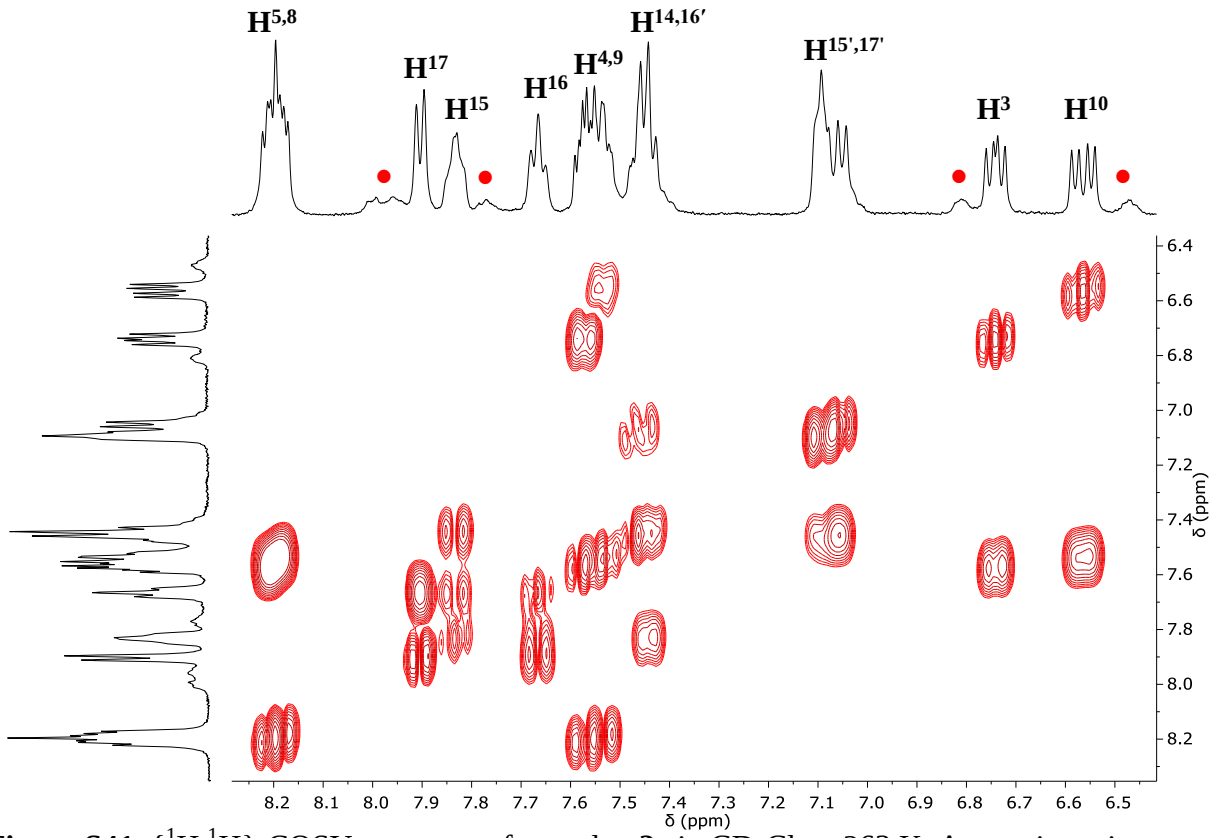

Figure S41. {^{1}H,^{1}H}-COSY spectrum of complex **2c** in CD_2Cl_2 at 263 K. Aromatic region.

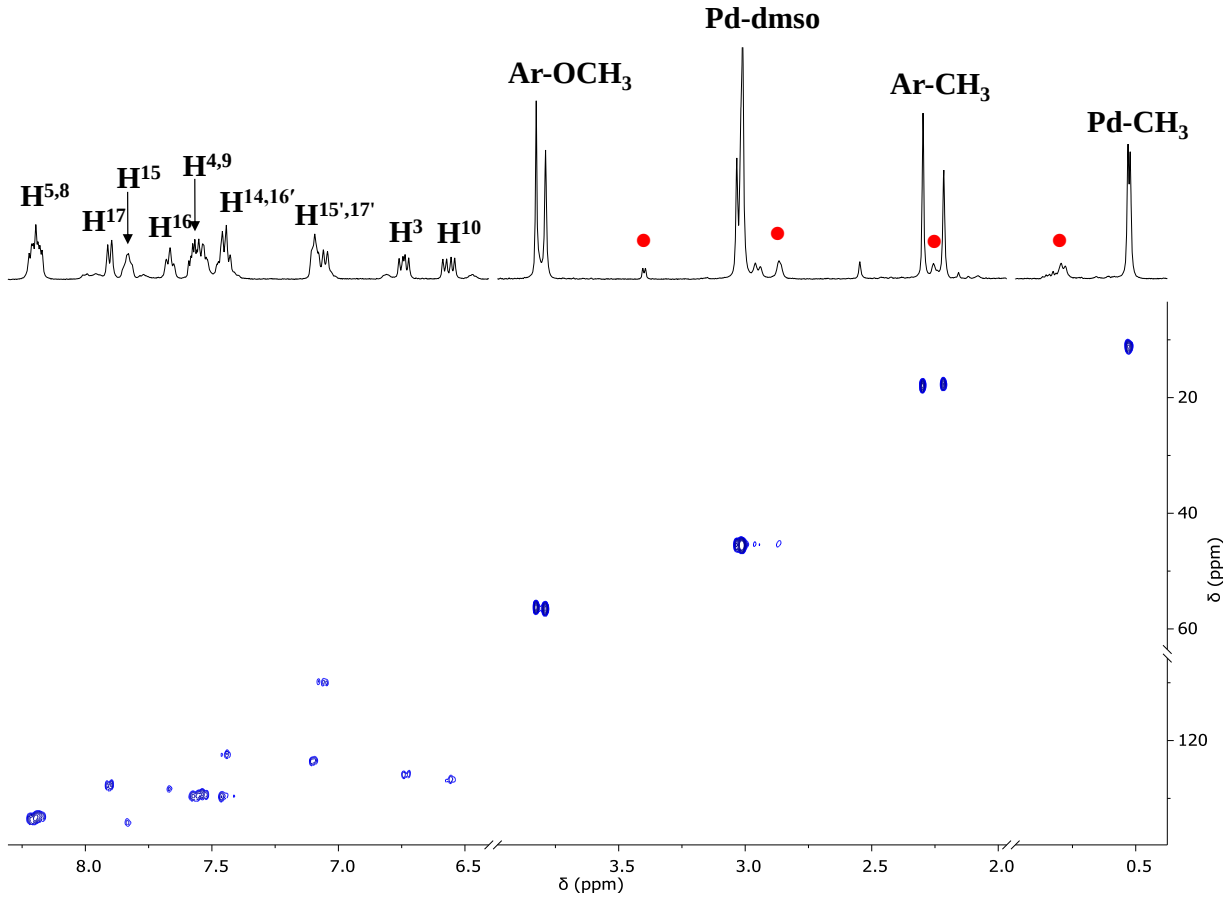

Figure S42. **{**^{1}H,^{13}C}-HSQC spectrum of complex **2c** in CD_2Cl_2 at 263 K.

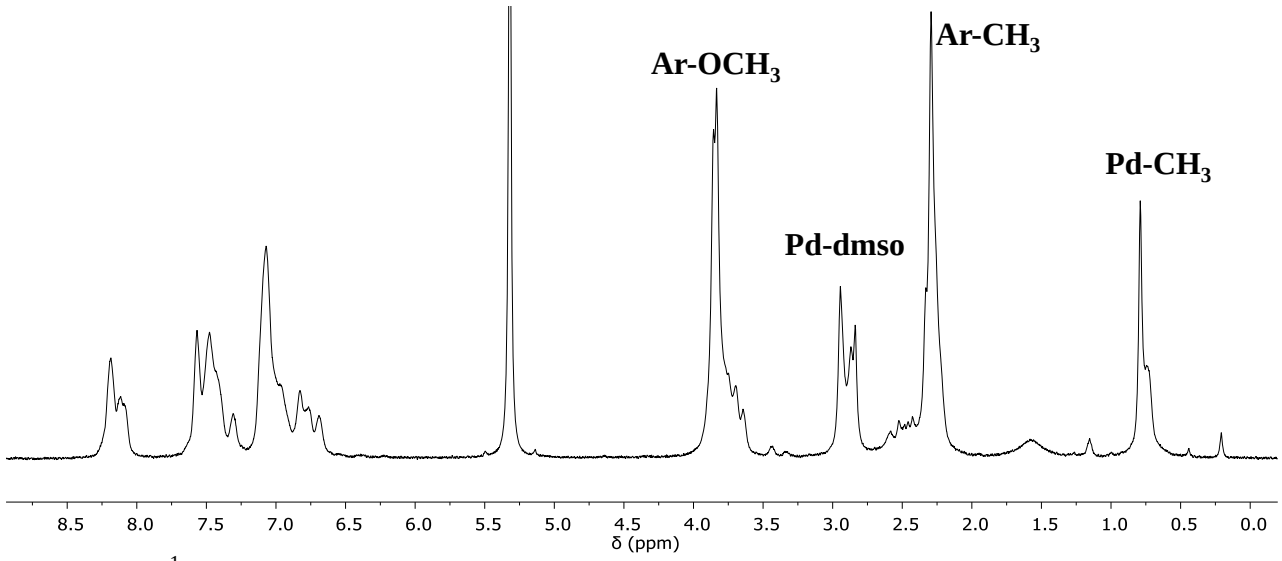

Figure S43. ^{1}H NMR spectrum of complex **3c** in CD_2Cl_2 at 298 K.

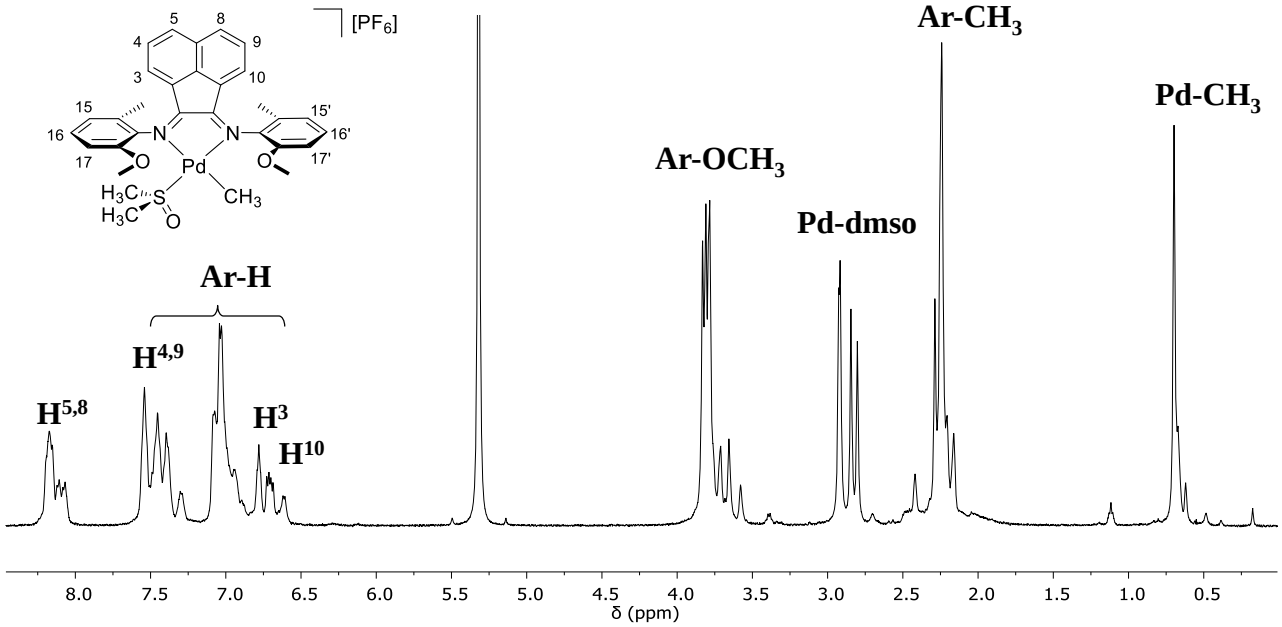

Figure S44. ^{1}H NMR spectrum of complex **3c** in CD_2Cl_2 at 233 K.

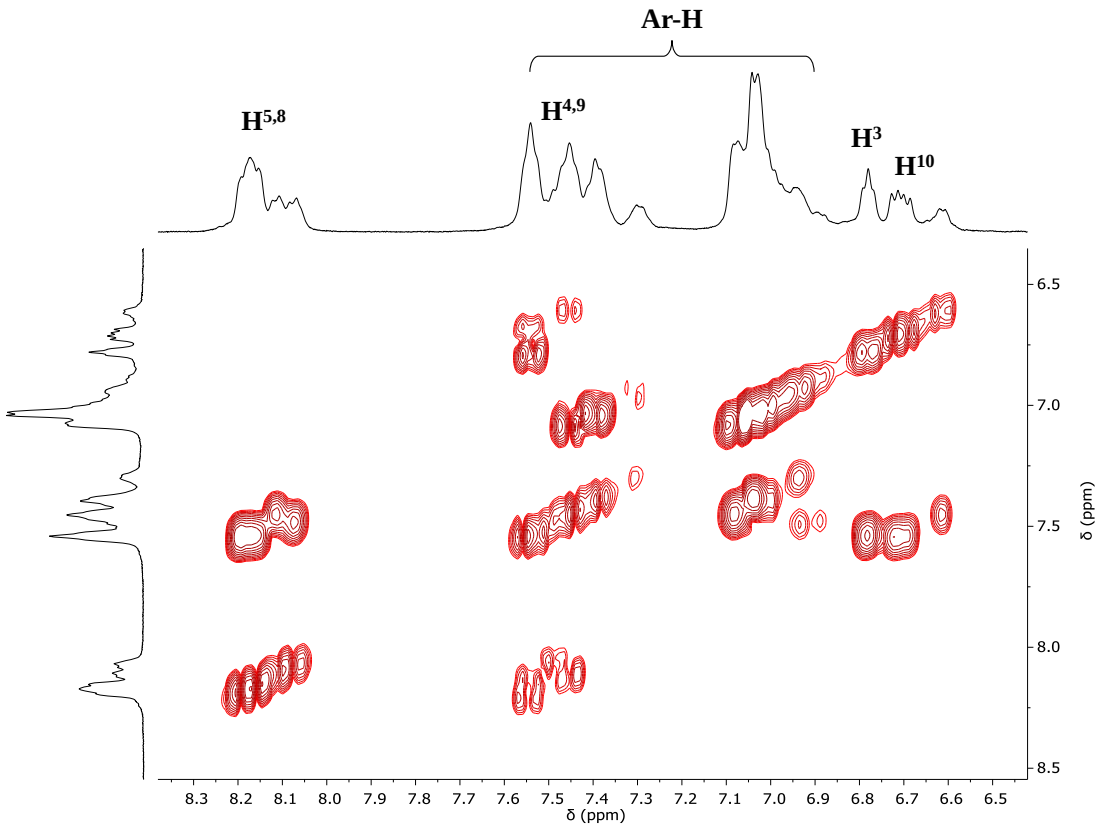

Figure S45. {^{1}H,^{1}H}-COSY spectrum of complex **3c** in CD_2Cl_2 at 233 K. Aromatic region.

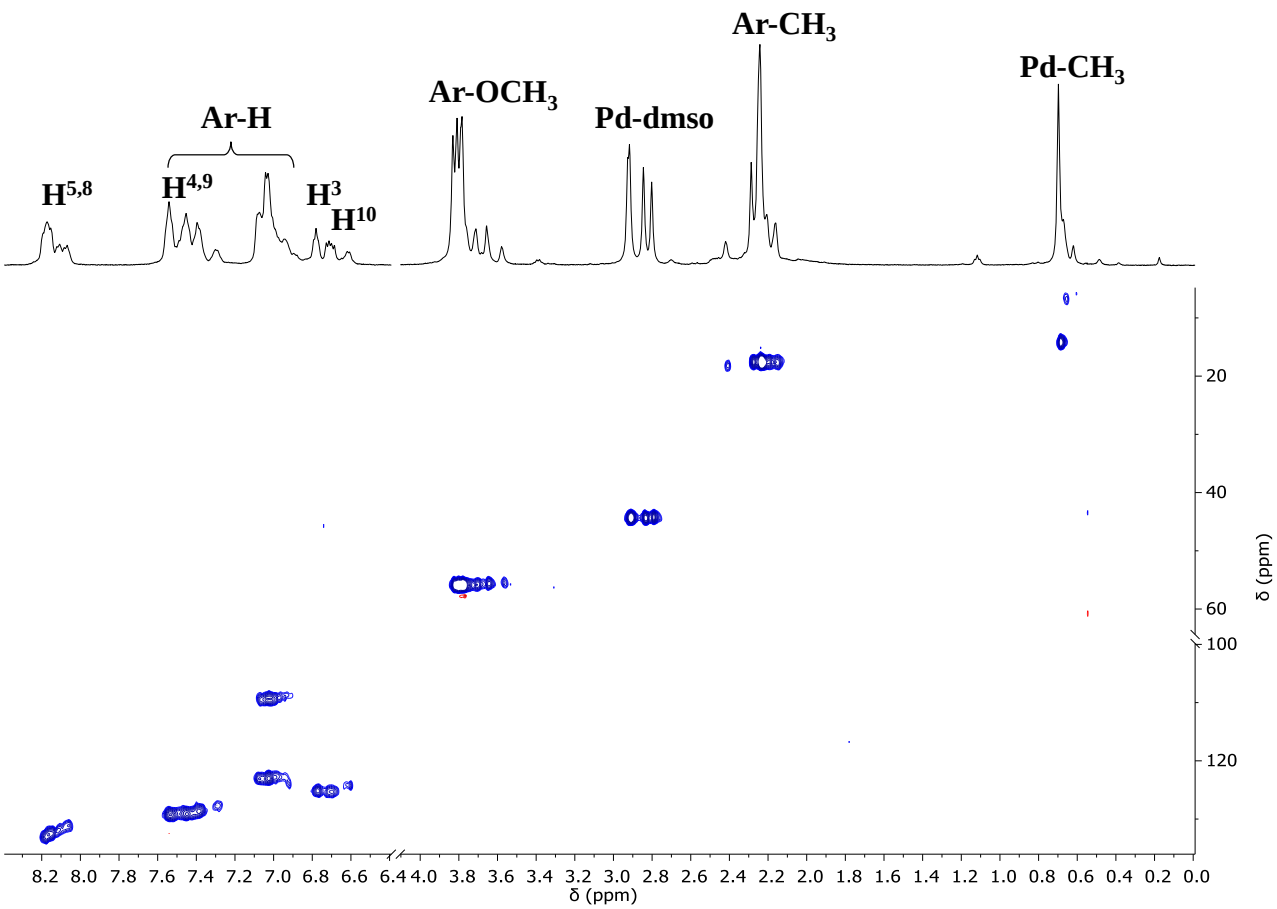

Figure S46. **{**^{1}H,^{13}C}-HSQC spectrum of complex **3c** in CD_2Cl_2 at 233 K.

Table S2. Ethylene/methyl acrylate cooligomerization: effect of the solvent.[a] Precatalyst: [Pd(CH_3)($NCCH_3$)(**1**)][PF_6].

Run	**Solvent**	Yield (mg)	g P/g Pd[b]	mol % MA[c]	Alkenes[d]
1	TFE[e]	157.1	70.4	25	C^{4-12}
2	CH_2Cl_2	16.5	-	-	C^{4-8}, C^{5-7}
3	toluene	24.3	-	-	-
4	methanol	10.6	-	-	-

[a] Reaction conditions: $n_{Pd} = 2.1 \cdot 10^{-5}$ mol, $V_{solvent}$ = 22 mL, V_{MA} = 1.130 mL, [MA]/[Pd] = 594, T = 308 K, $P_{ethylene}$ = 2.5 bar, t = 24 h; [b] isolated yield, productivity as g P/g Pd = grams of product per gram of Pd; [c] calculated by ^{1}H NMR spectroscopy on isolated product; [d] determined by GC/MS; [e] V_{TFE} = 21 mL.

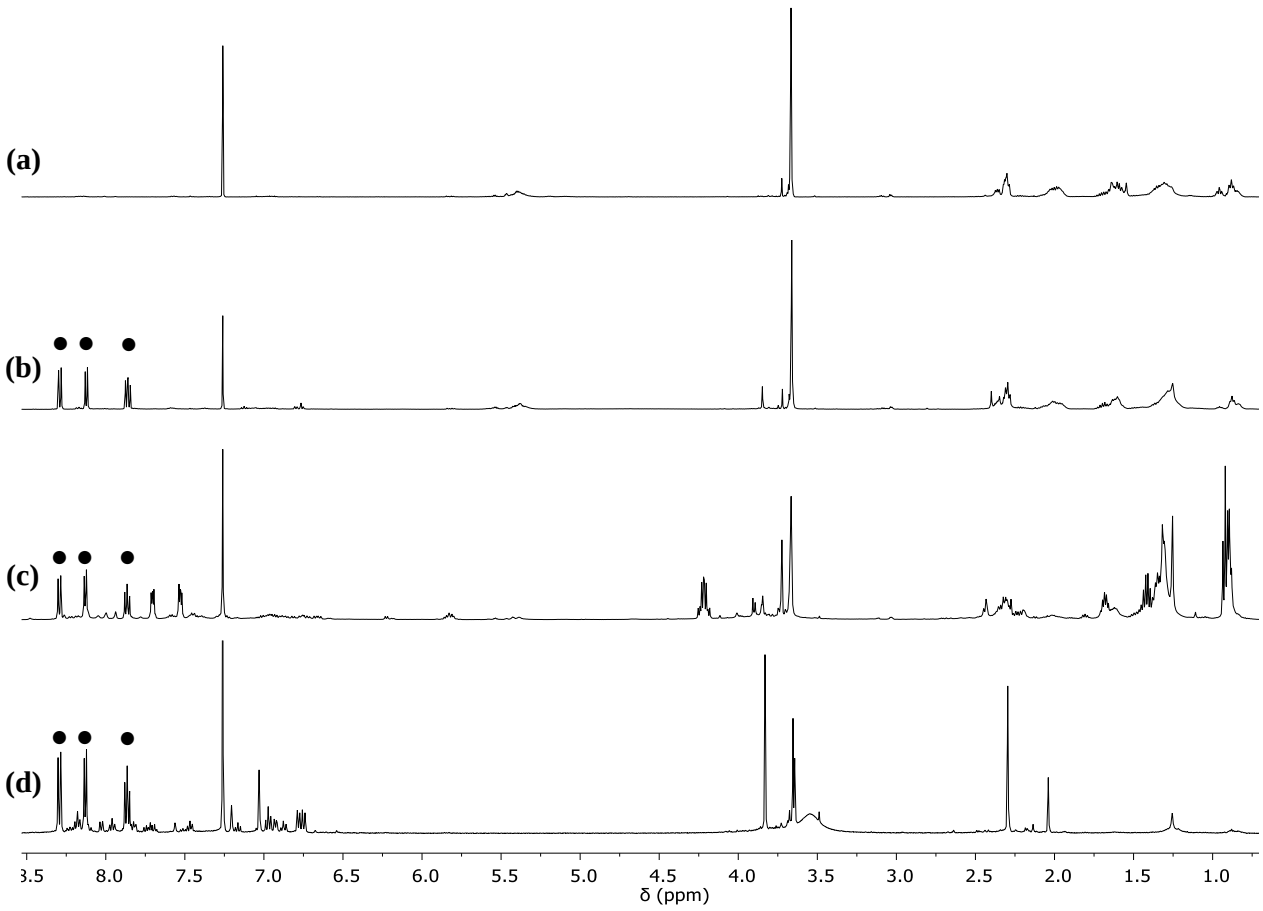

Figure S47. ^{1}H NMR in $CDCl_3$ at 298 K of the catalytic product obtained with **1b** in (a) TFE, (b) CH_2Cl_2, (c) toluene, (d) methanol. ● acenaphthenequinone.

GC/MS analysis of the formed higher alkenes

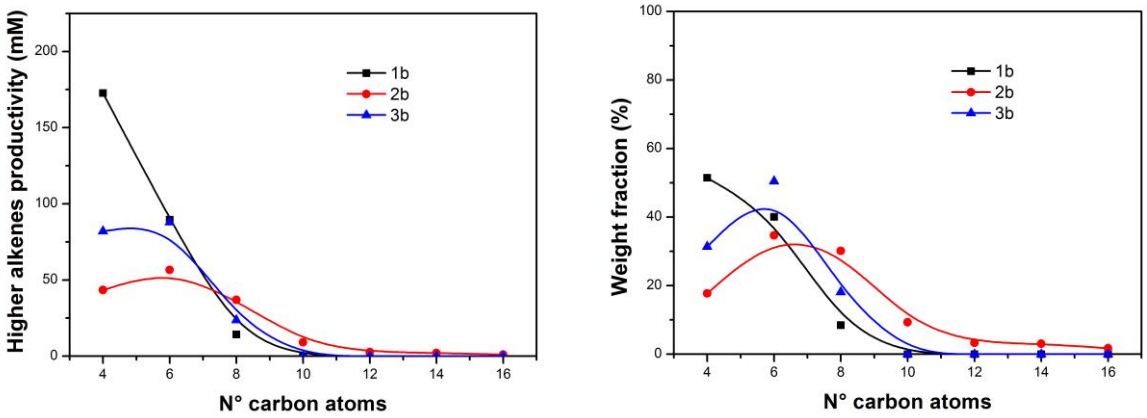

Figure S48. Results from GC/MS analysis of alkenes C^4-C^{16} for the CH_3CN-derived precatalysts, **1b-3b**.

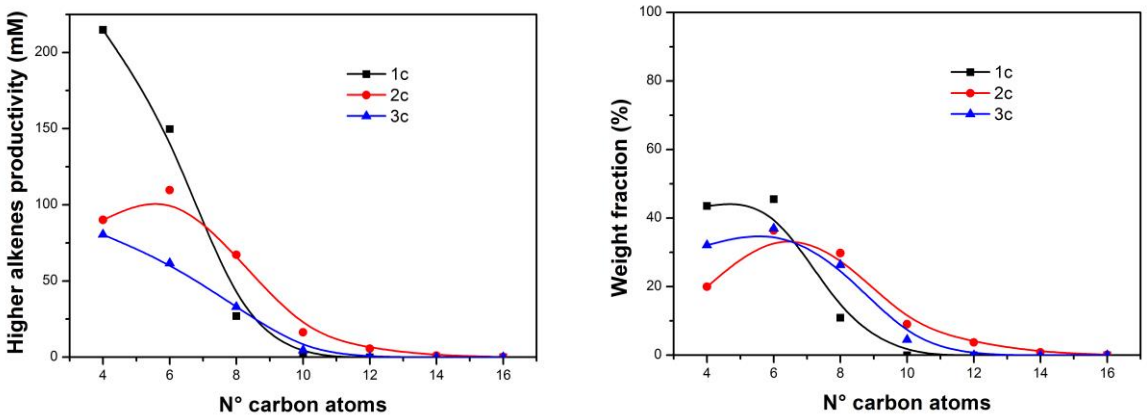

Figure S49. Results from GC/MS analysis of alkenes C^4-C^{16} for the dmso-derived precatalysts, **1c-3c**.

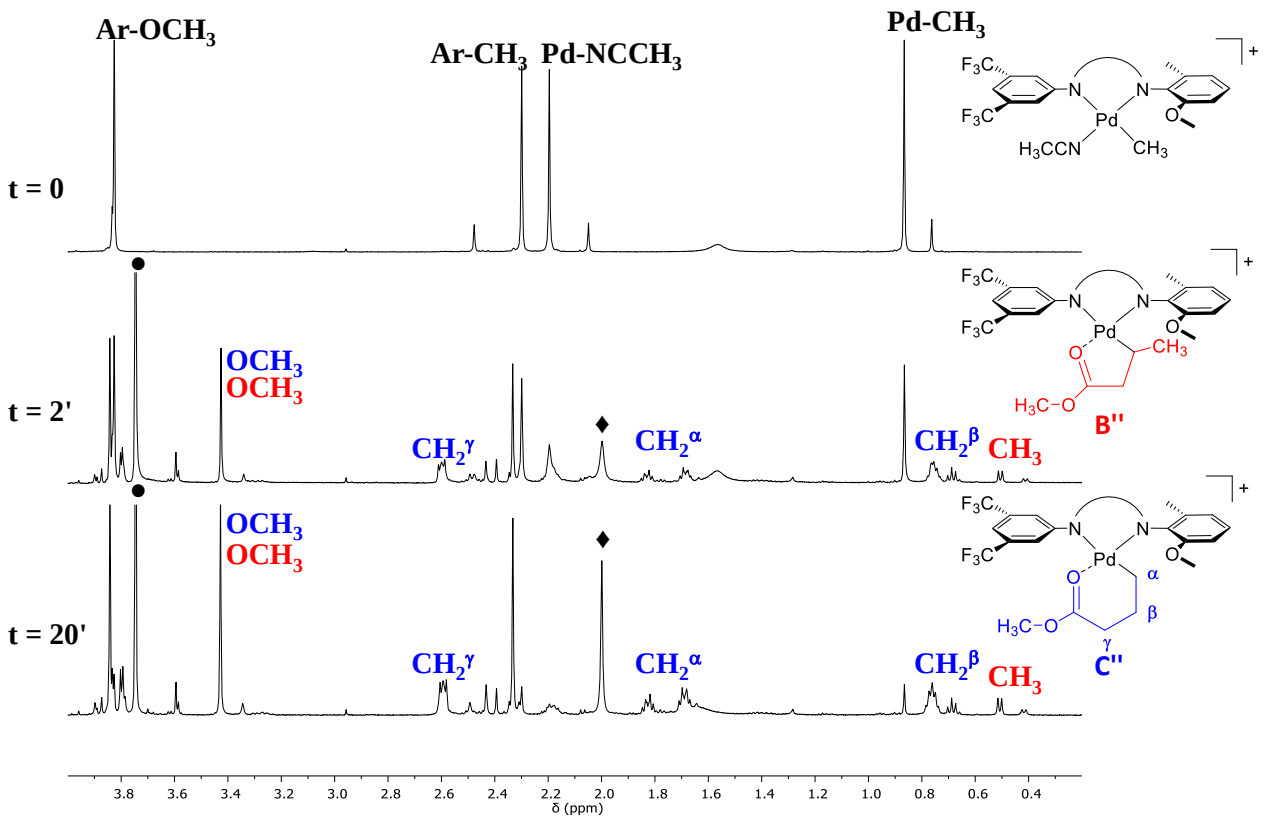

Figure S50. ^{1}H NMR in CD_2Cl_2 at 298K of the reactivity of **1b** with MA, aliphatic region, evolution with time. ● free MA; ♦ free acetonitrile. Only metallacyclic intermediates are shown.

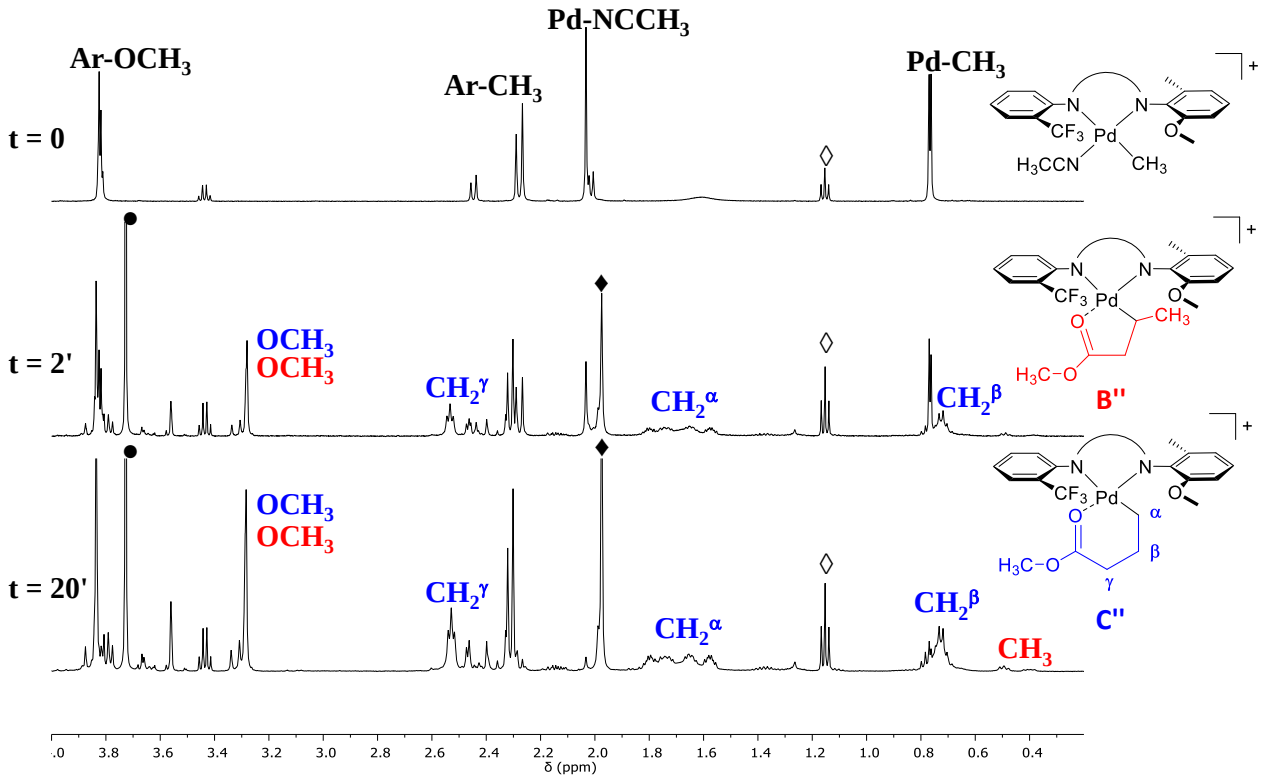

Figure S51. ^{1}H NMR in CD_2Cl_2 at 298K of the reactivity of **2b** with MA, aliphatic region, evolution with time. ● free MA; ♦ free acetonitrile; ◊ diethyl ether. Only metallacyclic intermediates are shown.

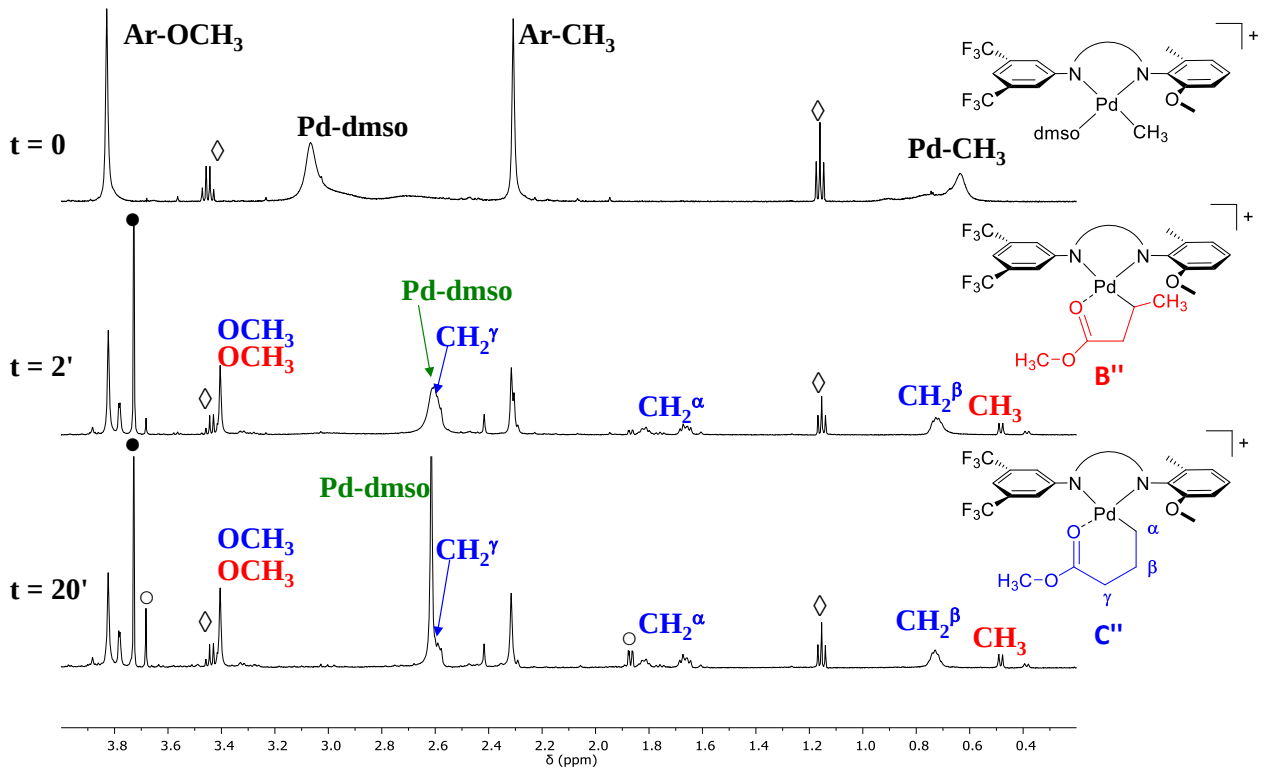

Figure S52. ^{1}H NMR in CD_2Cl_2 at 298K of the reactivity of **1c** with MA, aliphatic region, evolution with time. ● free MA; ◊ diethyl ether; ○ methyl crotonate. Only metallacyclic intermediates are shown.

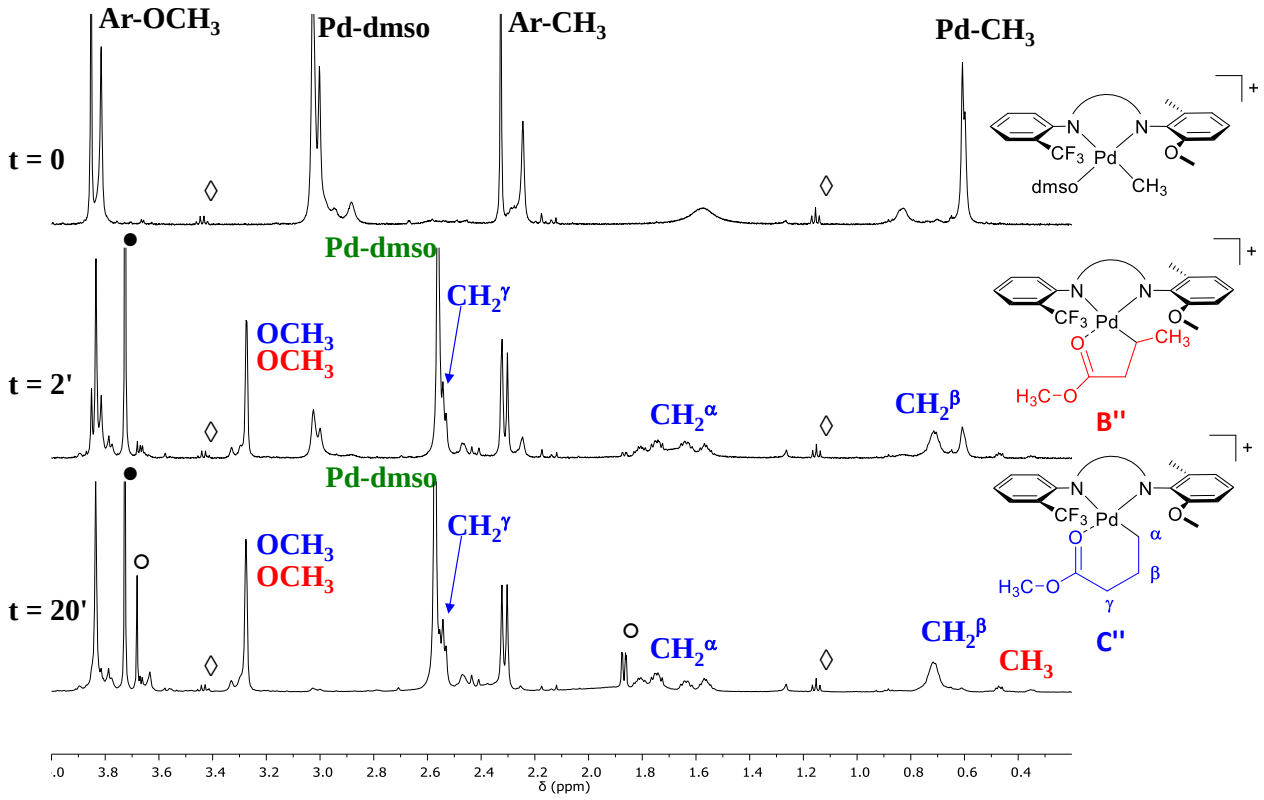

Figure S53. ^{1}H NMR in CD_2Cl_2 at 298K of the reactivity of **2c** with MA, aliphatic region, evolution with time. ● free MA; ◊ diethyl ether; ○ methyl crotonate. Only metallacyclic intermediates are shown.